EFFECT OF SCAFFOLD ARCHITECTURE AND MATERIAL ON STRESS SHIELDING PHENOMENA IN CONTACT REGION WITH A MANDIBLE HOST BONE; A FINITE ELEMENT ANALYSIS

Ammar Hussen Farag IDRES

2022
M.Sc. THESIS
DEPARTMENT OF BIOMEDICAL ENGINEERING

Thesis Advisor
Assist. Prof. Daver ALİ

EFFECT OF SCAFFOLD ARCHITECTURE AND MATERIAL ON STRESS SHIELDING PHENOMENA IN CONTACT REGION WITH A MANDIBLE HOST BONE; A FINITE ELEMENT ANALYSIS

Ammar Hussen Farag IDRES

T.C.
Karabük University
Institute of Graduate Programs
Department of Biomedical Engineering
Prepared as
M.Sc. Thesis

Thesis Advisor
Assist. Prof.Dr. Daver ALİ

KARABUK
January 2022

I certify that in my opinion the thesis submitted by Ammar Hussen Farag IDRES titled "EFFECT OF SCAFFOLD ARCHITECTURE AND MATERIAL ON STRESS SHIELDING PHENOMENA IN CONTACT REGION WITH A MANDIBLE HOST BONE; A FINITE ELEMENT ANALYSIS" is fully adequate in scope and quality as a thesis for the degree of Master of Science.

Assist.Prof.Dr. Daver ALİ .....
Thesis Advisor, Department of Medical Engineering

This thesis is accepted by the examining committee with a majority vote in the Department of Biomedical Engineering as a M.Sc. thesis. January 14, 2022

Examining Committee Members (Institutions)		Signature
Chairman	: Assoc.Prof.Dr. Hüccet KAHRAMANZADE (KTU)	Online
Member	: Assist.Prof.Dr. Daver ALİ (KBU)	.....
Member	: Assist.Prof.Dr. Kenan IŞIK (KBU)	Online

The degree of Master of Science by the thesis submitted is approved by the Administrative Board of the Institute of Graduate Programs, Karabuk University.

Prof. Dr. Hasan SOLMAZ .....
Director of the Institute of Graduate Programs

"I declare that all the information within this thesis has been gathered and presented in accordance with academic regulations and ethical principles and I have according to the requirements of these regulations and principles cited all those which do not originate in this work as well."

Ammar Hussen Farag IDRES

ABSTRACT

M.Sc. Thesis

EFFECT OF SCAFFOLD ARCHITECTURE AND MATERIAL ON STRESS SHIELDING PHENOMENA IN CONTACT REGION WITH A MANDIBLE HOST BONE; A FINITE ELEMENT ANALYSIS

Ammar Hussen Farag IDRES

Karabük University
Institute of Graduate Programs
Department of Biomedical Engineering

Thesis Advisor:
Assist. Prof.Dr. Daver ALİ
January 2022, 44 pages

All the scaffolds had a constant porosity of 80%. Also, three materials (Ti alloys, Mg, and PLA) were assigned for each model of scaffolds. Therefore, in this work, a total amount of twelve models was developed. Then, the models were investigated under biomechanical loads using finite element analysis. The von Mises stress in the scaffolds and contact surfaces with host bone was calculated to show the scaffold's performance under such loading. The analysis results showed that the pressure in the scaffold and its contact surface with the spongy bone are directly related to its stiffness. The highest stress was in the models with titanium and the lowest for the models with polymer material. There was no such relationship for stress at the contact surface of cortical bone with the scaffolds. Stress in these three areas showed significant

fluctuation with the change of scaffold architecture. The maximum von Mises stress in the scaffold was calculated in the models with cubic body center architecture. For both bone contact surfaces, the maximum von Mises stress appeared in models with Rhombicuboctahedron. The results of this study shed more light on the correct choice of scaffolds for orthopedic applications.

Key Words : Mandibular defect, Scaffold, Tissue engineering, Finite element analysis.

Science Code : 92504

ÖZET

Yüksek Lisans Tezi

İSKLE MIMARISI VE MALZEMESININ MANDIBULA KONAK KEMIĞI ILE TEMAS YÜZEYLERINDE GERILIME YIĞIMINA ETKISI; SONLU ELEMAN ANALIZI

Ammar Hussen Farag IDRES

Karabük Üniversitesi
Lisansüstü Eğitim Enstitüsü
Biyomedikal Mühendisliği Bölümü

Tez Danışmanı:
Dr.Öğr.Üyesi Daver ALİ
Ocak 2022, 44 sayfa

Doku mühendisliği tarafından geliştirilen iskeleler kullanılarak hasarlı kemiğin onarımı ve doldurulması ortopedik cerrahide ileri bir tedavi yöntemidir. İskeleler, trabeküler kemik yapısını taklit eden gözenekli malzemelerdir. İskeleler mimari ve malzeme açısından çok çeşitlidir. Bu çeşitlilik bazen hasarlı kemiği tedavi etmek için uygun iskeleyi seçmeyi zor bir süreç haline getirmektedir. Kemiğin yapısı çeşitli bölgelerinde farklı olması nedeniyle konak kemiğin ihtiyaçlarına uygun iskele seçimi daha da karmaşık hale gelmektedir. Bu nedenle iskelelerin mimarileri ve seçilen malzemenin onların biyomekanik yükler altında davranışlarını doku mühendisleri tarafından incelenmektedir. Bu çalışmada, bir çene kemiğindeki oluşan boşluğu doldurmak için octet, octahedron, cubic body center, and Rhombicuboctahedron mimariye sahio dört farklı iskele tasarlandı. Tasarımlanan tüm iskeleler, %80'lik sabit gözenekliliğe sahiptirler. Ayrıca, her bir iskele modeli için üç farklı malzeme (Ti

alaşımları, Mg ve PLA) seçilmiştir. Böylece, bu çalışmada toplam on iki model geliştirilmiştir. Daha sonra modeller, sonlu elemanlar analizi kullanılarak biyomekanik yükler altında incelenmiştir. İskelelerdeki ve konak kemikle temas yüzeylerindeki von Mises gerilmesi hesaplanmıştır. Analiz sonuçları, iskele ve süngerimsi kemiğin temas yüzeyinde meydana gelen gerilmenin iskele sertliği ile doğrudan ilişkili olduğunu göstermiştir. En yüksek gerilim titanium iskele modellerde, en düşük gerilim ise polimer malzemeli modellerde hesaplanmıştır. Kortikal kemiğin iskelelerle temas yüzeyindeki gerilme için böyle bir ilişki bulunmamıştır. Bu üç farklı bölgedeki gerilme, iskele mimarisinin değişmesiyle önemli dalgalanmalar göstermiştir. İskele mimari açısından maksimum von Mises gerilme kübik gövde merkezli mimarisine sahip modellerde hesaplanmıştır. Her iki kemik temas yüzeyi için maksimum von Mises gerilmesi, Rhombicuboctahedron'lu modellerde ortaya çıktı. Bu çalışmanın sonuçları, ortopedik uygulamalar için doğru iskele seçimine yönelik yenilikler katmıştır.

Anahtar Sözcükler : Alt Çene Kemği, İskele, Doku Mühendisliği, Sonlu elemanlar analizi.

Bilim Kodu : 92504

ACKNOWLEDGMENT

First of all, I would like to present my sincere gratitude and thanks to my advisor, Dr. Daver Ali, for his great interest, support, and advice in preparing this thesis and for sharing valuable information with me throughout this project and study.

Secondly, I would like to thank Assoc. Prof. Hüccet KAHRAMANZADE for sharing the mandible three-dimensional model.

I would like to sincerely thank my beloved best friend, soul mate, and wife Zeynep for her support during this study. Also, my parents have suffered a lot for assisting me in approaching this level of education in a foreign country and being patient about my absence beside them.

CONTENTS

Page

APPROVAL ii
ABSTRACT iv
ÖZET vi
ACKNOWLEDGMENT viii
CONTENTS ix
LIST OF FIGURES xi
LIST OF TABLES xiii
SYMBOLS AND ABBREVITIONS INDEX xiv

CHAPTER 1 1
INTRODUCTION 1
1.1 PROBLEM STATEMENT 1
1.2 OBJECTIVES 2
1.3 SCOPE OF STUDY 2
1.4 RESEARCH QUESTIONS 3

CHAPTER 2 4
LITERATURE REVIEW 4
2.1 ANATOMY OF THE MANDIBULAR BONE 4
2.2 BIOMECHANICAL OF THE MANDIBLE 8
2.3 HISTORY OF MANDIBULAR RECONSTRUCTION 9
2.4 METHODS FOR MANDIBULAR RECONSTRUCTION 9
2.4.1 Mandibular Reconstruction Plates and Screws 11
2.4.2 Non Vascularized Bone Grafting 11
2.4.2.1 Iliac Bone Reconstruction 11
2.4.2.2 Costochondral Rib 12
2.4.3 Vascularized Free Flaps 12
2.4.3.1 Donor bones as free Flaps 12

Page

2.4.4 Modular Endoprosthesis Replacement 13
2.4.5 Scaffold Tissue-Engineering 14
2.4.5.1 3D Scaffolds 15
2.4.5.2 Scaffolds Materials and Fabrication Methods 16
2.5 ART OF BONE SCAFFOLD DESIGN 17

CHAPTER 3 19
METHODOLOGY 19
3.1 MATERIALS 19
3.1.1 MANDIBLE BONE AND CAD MODELS 19
3.1.2 SCAFFOLD MODELS 20
3.1.3 FINITE ELEMENT ANALYSIS (FEA) 20
3.1.4 MESHING THE MODELS 21
3.1.5 BOUNDARY CONDITION 22
3.1.6 Eq. von Mises STRESS 23

CHAPTER 4 25
RESULTS AND DISCUSSION 25
4.1 RESULTS RELIABILITY 25
4.2 DISCUSSION 30

CHAPTER 5 35
SUMMARY 35

REFERENCES 37

RESUME 44

LIST OF FIGURES

Page

Figure 2.1.The Mandible Bone from above and from the right side Shows the cortical 5
Figure 2.2. Anatomy of the Mandibular Bone 5
Figure 2.3. Mandibular Masseter Muscle Superfical 6
Figure 2.4. For Masseter Muscles and 2 for Temporalis Muscles 7
Figure 2.5. Torsion, Transverse Benning and Sagittal Bending 8
Figure 2.6. HCL Mandibular defects Classification 10
Figure 2.7. Mandibular Reconstruction Progras by Plates and Screws 11
Figure 2.8.a) Modular Endoprosthesis Replacement illustration, b) Endoprosthesis before implanting. 14
Figure 2.9. Mandible repaired by scaffold tissue engineering 15
Figure 3.1. a) CAD model and its b) exploded view of the parts. 19
Figure 3.2. Scaffolds CAD models and their uni tcells a) Octet 300 μm , b) Octahedron 440 μm , c) Cubic Body Center 390 μm and d) Rhombicuboctahedron 340 μm. 20
Figure 3.3. Whole model mesh and refined mesh in the scaffold-bone contact area. 21
Figure 3.4. The muscle force and bite force in the FEA model. 22
Figure 3.5. Stress Tensor Element. 24
Figure 4.1. The total deformation of the mandible under the muscles and bite force. 25
Figure 4.2. Von Mises stress contour in Rhombicuboctahedron-Ti n scaffold. 26
Figure 4.3. The calculated max. vM. s (MPa) in the scaffolds. 26
Figure 4.4. vM.s distribution in cancellous bone contact surface in Rhombicuboctahedron-Ti model. 27
Figure 4.5. The max. vM. s (MPa) in cancellous bone contact surface with scaffold. 28
Figure 4.6. vM. s contour in cortical bone and scaffold contact area for the Rhombicuboctahedron-Ti model. 29
Figure 4.7.The max. vM. s on the cortical bone contact surface with scaffold for all the models. 29
Figure 4.8. vM.s contour for scaffolds with Ti alloy material. a) Octet, b) Octahedron, c) Cubic body center, and d) Rhombicuboctahedron. 31

Page

Figure 4.9. vM.s contour on cancellous bone contact surface for the models with Ti alloy scaffolds. a) Octet, b) Octahedron, c) Cubic body center, and d) Rhombicuboctahedron. 32

Figure 4.10. vM.s contour on cortical bone contact surface for the models with Ti alloy scaffolds. a) Octet, b) Octahedron, c) Cubic body center body center and d) Rhombicuboctahedron. 33

LIST OF TABLES

Page

Table 3.1. Material properties for the FEA models. 21
Table 3.2. Mesh statistics of FEA models..... 22
Table 3.3. The applied muscle and bite forces (N) in FA. 23

SYMBOLS AND ABBREVITIONS INDEX

SYMBOLS

σ : Normal stress

τ : Shear stress

Mg : Magnesium

Ti : Titaniyum

PLA : Polyglycolic acid

ABBREVITIONS

TE : Tissue Engineering

TEMJ : Temporomandibular Joints

MP : Medıal Pterygoid

RFFF : Radial Forearm Free Flap

PM : Pectoralis Major Myocutaneous

ECM : Extracellular Matrix

3D : Three Dimensional

CAD : Computer Aided Design

CT : Computed Tomography

MRI : Magnetic Resonance Imaging

PLA : Polyglycolic acid

CHAPTER 1

INTRODUCTION

Only witches could tell somebody who lost his leg bone that she can replace it with a new one, but that is unfortunately not real at all. A century ago, nobody would believe that if somebody told you the same thing.

After decades of research in medical history, many attempts have been made to heal the loss of body organs [1]. Tissue engineering has made a significant improvement to treat whether xenotransplantation or donating organs from other people. However, allotransplantation and xenotransplantation are not available enough to satisfy the massive demand for organs worldwide [2].

Recently, thanks to three-dimensional (3D) additive manufacturing methods and significant advances in tissue engineering, synthetic materials were developed to replace and heal damaged organs [2]. Many studies showed that using a 3D scaffold is a good alternative instead of transplantation [3–5].

1.1 PROBLEM STATEMENT

Designing and selecting a proper scaffold for bone defects is acritical in tissue engineering. Because bone tissue is rigid and bears mechanical loads, developing an alternative implant that can perform its functions requires the consideration of many parameters. One of the bones that can damage due to old age, illness, or accident is the mandibular bone. Mandible bone plays a vital role in the body's digestion system. Bite force can vary between 40-400 N during feeding food [6]. Also, the mandibular bone moves when it speaks, and this causes tensions in its structure. Therefore, selecting a suitable implant that can help a patient to achieve his/her healthy eating mechanism is essential. Bioceramics such as hydroxyapatite and tricalcium phosphate are good

candidates for filling mandibular bone defects [7]. Recently porous scaffolds with regular architectures and controllable mechanical properties got more attention as bone replacement implants thanks to their more biocompatible characteristics [8,9]. Some studies investigated filling mandible bone defects using porous scaffolds [10,11]. Scaffolds are materials with porosity that help bone regeneration spatially when the bone defect is significantly large [12].

Scaffolds' mechanical and biological behavior depends on their architecture, porosity, and materials. For example, increasing the porosity of scaffolds improves cells' bioactivity within them but causes decreasing in their strength under biomechanical loads [13]. As a main mechanical property, scaffolds' effective elastic modulus should be considered because a low elasticity cannot tolerate biomechanics loads, and an excessively high elastic modulus can cause the undesirable stress-shielding phenomenon. Then, selecting a proper scaffold with enough strength and avoiding stress shielding phenomena is a challenge in bone tissue engineering [14]. In this study, we used a mandible bone with a defect to investigate the effect of scaffolds architecture and material on the stress distribution at bone-scaffold contact sites using finite element method.

1.2 OBJECTIVES

The objectives of this thesis are

1. This study uses a mandible bone model with a fixed defect size in the symphysis area.
2. The defect was filled using four scaffolds with different architecture.
3. Three different materials were assigned to scaffolds to test the effect of scaffolds stiffness on stress distribution in contact surface with host bone.
4. A total of twelve models were analyzed numerically in this study.

1.3 SCOPE OF STUDY

The results of this study, with all its limitations, are a step forward in elucidating and better understanding the behavior of scaffolds under actual loading conditions. This

study paves the way for further studies on selecting and designing more compatible scaffolds with host bone.

1.4 RESEARCH QUESTIONS

- How can we use computational simulation in biomechanical problems analysis?
- How do the architecture and material of a scaffold affect the load transmission in contact surfaces?
- How to find the most appropriate scaffold architecture for the mandible bone defects replacements?

CHAPTER 2

LITERATURE REVIEW

2.1 ANATOMY OF THE MANDIBULAR BONE

Without bones, the human body will not move correctly [2]. In terms of cellular structure and functions, it comprises osteoblasts, osteocytes, and osteoclasts, the three types of bone cells. Osteoblasts can create bone and generate matrix proteins in a cubic body center shape. Osteocytes are cells that maintain the health of bone tissue and transport chemicals. Osteoclasts are bone-destroying cells with resorption functions. Osteoclasts destroy trabeculae or compact portions during bone production, while osteoblasts create new bone tissue [2,15].

Bone is made from two distinguished parts, as shown in figure 2.1. Cortical type for the outside layer of the bone is more complex than the density of the bone mass cell. These cells are known as the microscopic columns (osteons), which are made up of the layers of osteoblasts and osteocytes. The second type is the cancellous bone which has the trabecular network with a highly porous ratio that allows blood vessels and narrow to pass through. Trabecula is orientated toward the biomechanical pressure distribution in bone and is considered the fundamental unit of the cancellous bone [11,15–17].

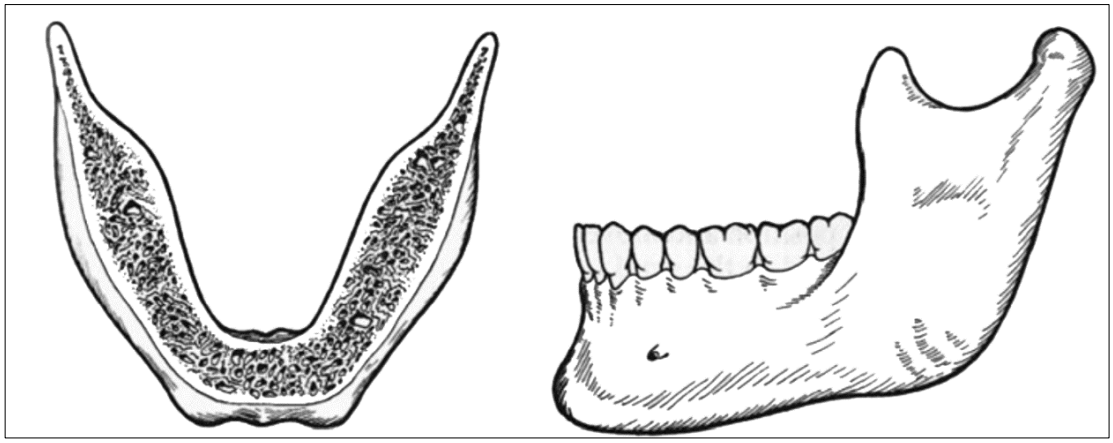

Figure 2.1. The Mandible Bone from above and from the right side Shows the cortical outside part of the bone and insider spongey part which is the cancellous [17].

As shown in figure 2.2, the mandibular bone is simply the lower jaw bone that takes the shape U in the human skeletal system. Its end edges join the muscles of the mastication (temporomandibular) [2]. The mandibular bone consists of 5 connected bone sections, 1, body (Corpus), 2 the symphysis, which is located in the front part of the mandibular and connects the two sides of the right and left part of the mandibular,3 alveolar bones, which are located under the teeth. Its job is to sustain the teeth during chewing [17].

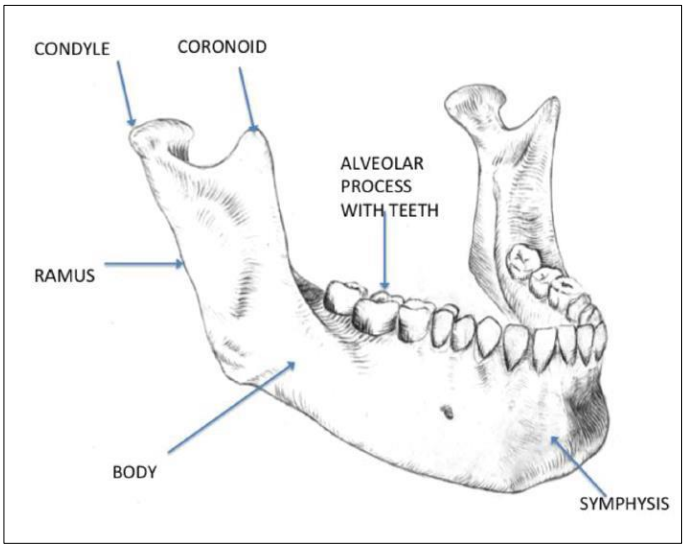

Figure 2.2. Anatomy of the Mandibular Bone [17].

Anatomy of the mandible showing Symphysis, Body, Ramus, Condyle, Coronoid and Alveolar Process with Teeth (figure 2.2) [17].

It is well known that the bones cannot be moved by themselves. There must be muscles to help them out to make the jawing process. There are three groups of the attached mandibular muscles [18].

Masticatory muscles consist of four muscles (figure 2.2).

1. MP Medial Pterygoid, helps for closing the mandible (figure 2.3, 2.4)
2. lateral Pterygoid, helps for opening the mandible
3. Masseter helps for closing the mandible
4. Temporalis, helps for closing the mandible

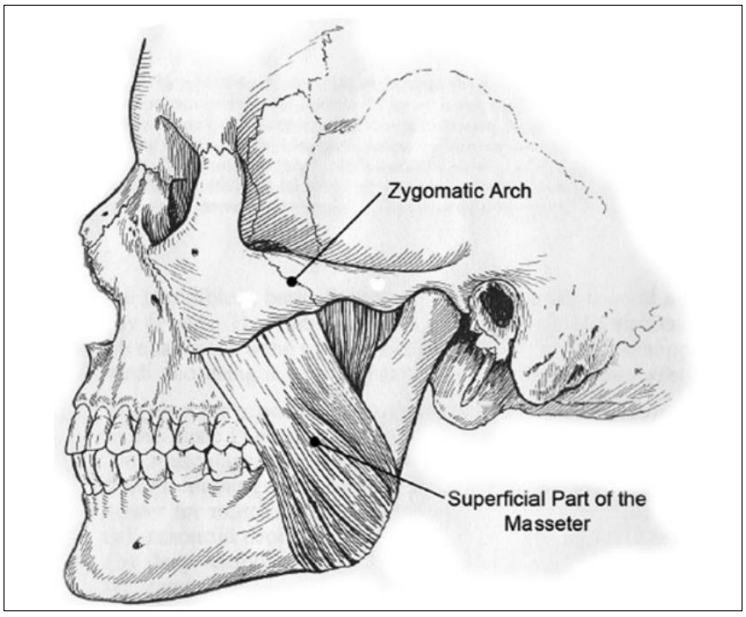

Figure 2.3. Mandibular Masseter Muscle Superfical [2].

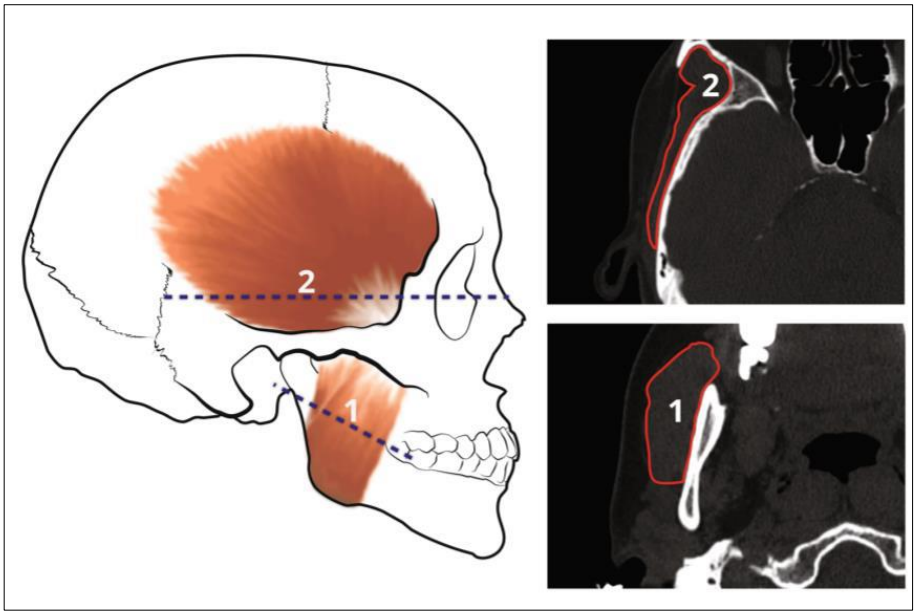

Figure 2.4. For Masseter Muscles and 2 for Temporalis Muscles [19].

Sprahyoid muscles have a critical role in some functions of the opening process of the mouth and swallowing mylohyoid, hyoglossus, genioglossus, digastric muscles. Muscles connected to the mandible and taking action for the facial expression are buccinators, depressors, anguli oris, and mentalis [20].

As mentioned above, the mandible consists of two bone surfaces: the cortical bone and the cancellous bone. Cortical bone is stiff and dense, but the thickness depends on the area, and in some sites, there is only cortical bone. The cancellous bone or the marrow is surrounded by cortical bone has a spongy and porous structure. The alveolar processes as part of ramus are good examples of the cancellous [17].

Mandible bone attaches to the skull through mastication muscles and the temporomandibular joints. This muscle and joint attachment combination keeps mandible bone in its proper positions and ables people to speak and chew. The temporomandibular upper and lower joint spaces are split by the articular cartilage, which is for the collagen fibrils capsule [15,17, 20, 21]

The muscles mentioned above, and joints control the movement of the bone. Mainly two types of movement in the mandible can be observed. The first movement is rotation which is about a hinge for the first 20 mm then followed by a translation, which is primarily influenced by the action of the lateral pterygoid muscle drawing the whole condyle to the front and out of the glenoid fossa onto a portion of the temporal bone's zygomatic process. Due to the articular eminence, a projection on the condyle restricts the forward mobility of the joint [15, 17, 20, 21].

2.2 BIOMECHANICAL OF THE MANDIBLE

The mandible is a bone that simultaneously experiences tensile and compression loading. An area of tension exists on the alveolar region of the mandible during function, while a domain of compression exists on the lower part of the bone’s edges [17, 19].

The mandible bends in a sagittal plane when the mastication muscles contract; this is caused by the vertical component of the muscle forces happening along the sagittal plane, joint response forces, and chewing motion reaction forces. The result is a stretching zone at the lower boundary and a compression zone at the alveolar portion (figure 2.5) [17].

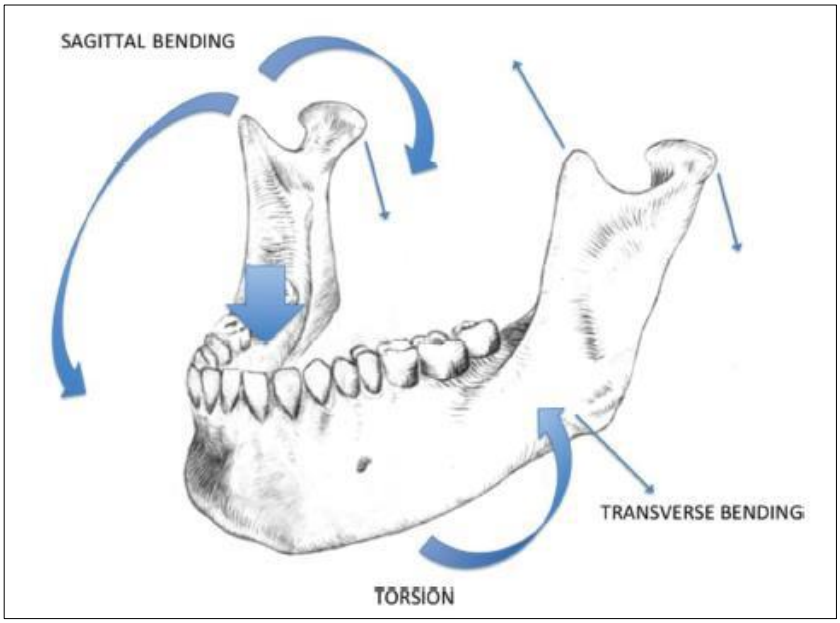

Figure 2.5. Torsion, Transverse Benning and Sagittal Bending [21].

2.3 HISTORY OF MANDIBULAR RECONSTRUCTION

From 1860 onwards, orthopedists began mandibular repair with early applications of bone grafts from various bones for small or large defects [22]. In surgical treatment, using a bone graft is a popular method for fusions, fracture repair, and the rebuilding of skeletal defects. The translation of bone from a member to another site in the same patient is known as autologous transplant [23]. Also, restoring a fractured mandible bone with a prosthetic appliance and metal materials was common in orthopedics applications [24, 25]. Other scientists suggested celluloid silver and hard rubber materials instead of metal plates [21]. With some emerging failures in the earlier materials, new materials such as Vitallium, stainless steel, and titanium were suggested for such applications [26, 27].

Scientists from World War II, such as Blocker and Stout, have emphasized the advantages of autografts, such as the tibial, rib, and iliac, which effectively reconstruct the mandible [28]. Wersal et al. looked at the use of split-rib grafts for mandible rebuilding following Blocker and Stout's study's results [29].

In 1986, (SOFF) or Scapular used the osteocutaneous free flap method in head and neck bones treatment [30]. Followed by, in the same year, the method was used by Hidalog and David A to transfer the fıbular autograft for the mandible restoration [31].

Therefore, defects in mandibular area are summarized as
1- Bone defects [21].
2- Soft Tissue such as skin or muscles [32].
3- Composite defects with bone and soft tissue [20].

2.4 METHODS FOR MANDIBULAR RECONSTRUCTION

A patient with mandibular defects who needs restoration is always looking for three things to recover and return to normal. Firstly, and more importantly, eating and talking without disturbances or extraordinary difficulties. Secondly, maintaining the ability to breathe throughout the airways during different activities and conditions.

Thirdly, the face esthetics and appearance without any abnormalities. Therefore, it is recommended to check if the restoration will aim to achieve these goals [21].

Based on position and extent, mandibular defects are categorized into three types: frontal mandible, posterior mandible, and ramus/condyle abnormalities. The assortment of mandible defects was introduced by Jewer et al. and then updated by Boyd et al. Defects in the center of the jaw bone are called ‘’C’’, for side parts without the condyle are referred to as ‘’L’’ and with condyle is referred as H. For defects in two or three places, the name goes as ‘’C, L, H, LC, HC, LCL, HCL’’ and HH (Figure2,6) [33,34].

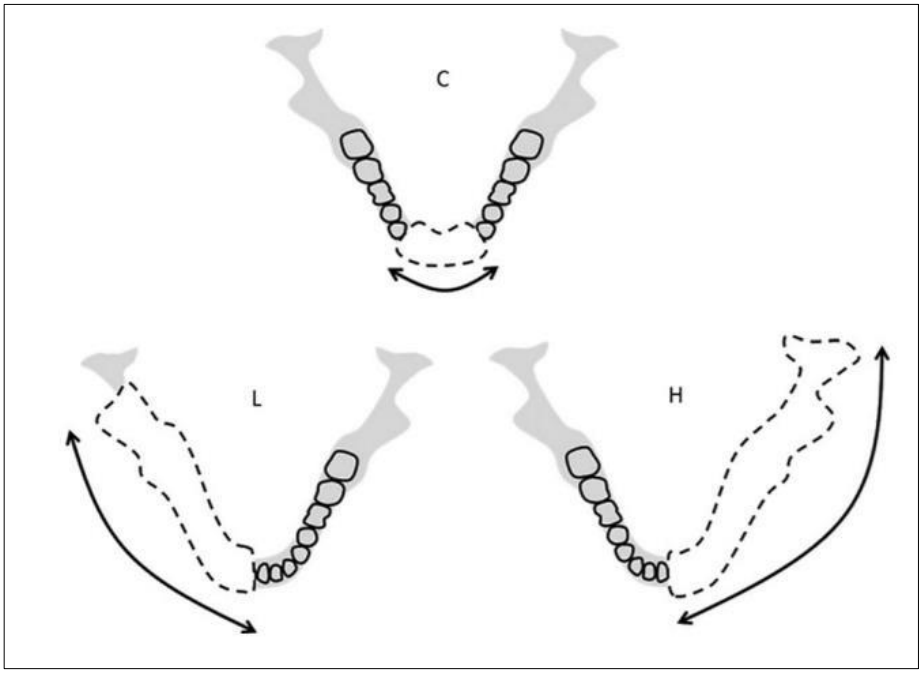

Figure 2.6. HCL Mandibular defects classification [34].

Generally, for a successful bone replacement or grafting, there are prerequisites such as proper and right fixation, blood supplilabity to the area, healthy bone tissue surrounding the transplantation, and contact between the affected bone area and the graft [35].

2.4.1 Mandibular Reconstruction Plates and Screws

One of the most famous and popular ways to rejoin a fractured bone is the plates and screws system. These plates and screws are primarily made from metals such as Stainless steel, Vitallium, and Titanium [36].The plate and screw fixation helps defected bone heal by forming a vascularized new bone tissue through the damaged bone and gaps (Figure 2.7).

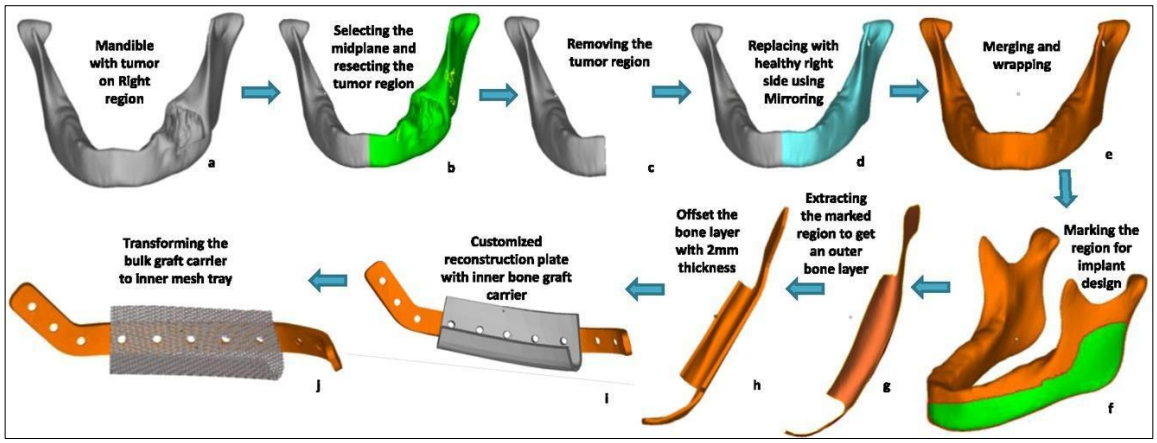

Figure 2.7. Mandibular Reconstruction Progras by Plates and Screws [37].

2.4.2 Non-Vascularized Bone Grafting

This type of bone defect treatment option is preferred for minor defects, provided that they do not lose any soft tissue or in tiny amounts. It is done by harvesting the donor bone to be replaced in the defected area of the mandible [29].

The donor site could be as following;

2.4.2.1 Iliac Bone Reconstruction

Bone restoring by using iliac bone is mainly used for cancellous bone defects. The harvested cancellous bone is an excellent platform for implantation [38].

2.4.2.2 Costochondral Rib

Mandibular condyle decfects can be replaced by costochondral graft for children and teenagers [39]. However, sometimes the replaced bone shows an undesired excessive growth [40].The rib and iliac crest are popular non-vascularized bone transplant donor sites. Thus, the rib can be used as a split rib transplant or a full rib graft [24, 29].

2.4.3 Vascularized Free Flaps

In this method, the vascularized bone is replaced without any interaction in the healing process within the host bone. There are now many donor locations for vascular bone flaps and soft tissue. In an ideal situation, the donor bone must be long enough to fill the gap while being wide and tall enough to support endosteal implants and endure the mastication loads when eating. The vascularized free flaps reconstruction method is more effective in biomechanical loads transfer [17].

2.4.3.1 Donor bones as free Flaps

Fibular free flap

A fibular free flap is recognized as the most donatable bone in the body for mandible reconstruction due to the following reason;

1- This bone blood network is available from endosteal and periosteal branches which allow surgeons to osteotomies the bone as segment location [17].
2- Approximately the length of the fibular is 25 cm which is for sure longer the donor site of the mandibular in contrast [17, 31, 41, 42].
3- Supply the cortical bone which is needed for repairing abnormalities across the midline section [17].

Radial Forearm Free Flap RFFF

It provides for a thin and pliable amount of skin. The length that this bone cover is between 10 – 12 cm which is 40% of both need to be cured [43].

Scapula Free Flap

One single flap can cover a reconstructıon defect of 11- 14 cm including the subscapular artery [44].

The Pectoralis Major Myocutaneous Flap (PM)

The PM flap is taken from the Pectrolis Myocutaneous region of the body to replace the lower third of the face and neck. It plays a useful role for the floor of the mouth which is caused generally by traumatic defects [45].

Iliac Crest Free Flap

This bone has many features to be implanted due to its high value of cancellous bone with enough height and thickness. As for the illiace crest, it is chosen for usage because it from resemblance to the hemi mandible opening osteomies in the iliac bone enables reliable anterior mandibular defect restoration [46].

2.4.4 Modular Endoprosthesis Replacement

This approach focuses on removing the diseased part of the bone with artificial fixation that remains as a bone supporter with a modular system that combines components to allow flexıbility long-term applications (figure 2.8) [47].

An endoprosthesis is mainly a metallic part inserted into the mandibular evacuated region. To accelerate implant and host bone joining, a bioceramic cement coating on the implant and bone contact region also would be helpful. Screw fixing is not required because the implant length is adjustable and can fit the bone gap. Meanwhile, a locking system links the implant segments together [48].

Using modular endoprosthesis for restoring an alloplastic mandibular is considered a unique way [49,50]. However, there were a few particular hurdles to overcome while using this reconstructive approach on the mandible bone because the mandible is a curved bone with teardrop shape cross-sections [50].

A

B

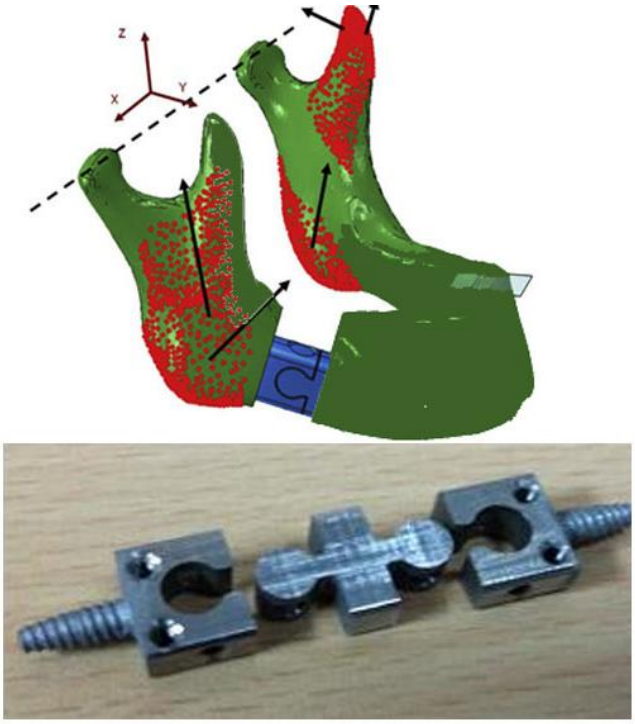

Figure 2.8. a) Modular endoprosthesis replacement illustration,
b) Endoprosthesis before implanting.

2.4.5 Scaffolds and Tissue Engineering

Microvascular bone flaps, both vascularized and non-vascularized with all the advantages, show some drawbacks. The donor site availability is rare and limited compared to defect size and number. Also, the donated bones' form does not satisfy the needed geometry and morphology, leading to an unpleasant appearance in the patient's face after the operation. Moreover, the setback that arises from the donor sites due to the loss of bone is another side effect. These disadvantages have led scientists to look for alternatives for bone flap methods [31, 41 ,45, 46].

Scaffolds are the latest generation of materials and structures recommended in orthopedics to treat bone failure, [15] as shown in the steps in figure 2.9.

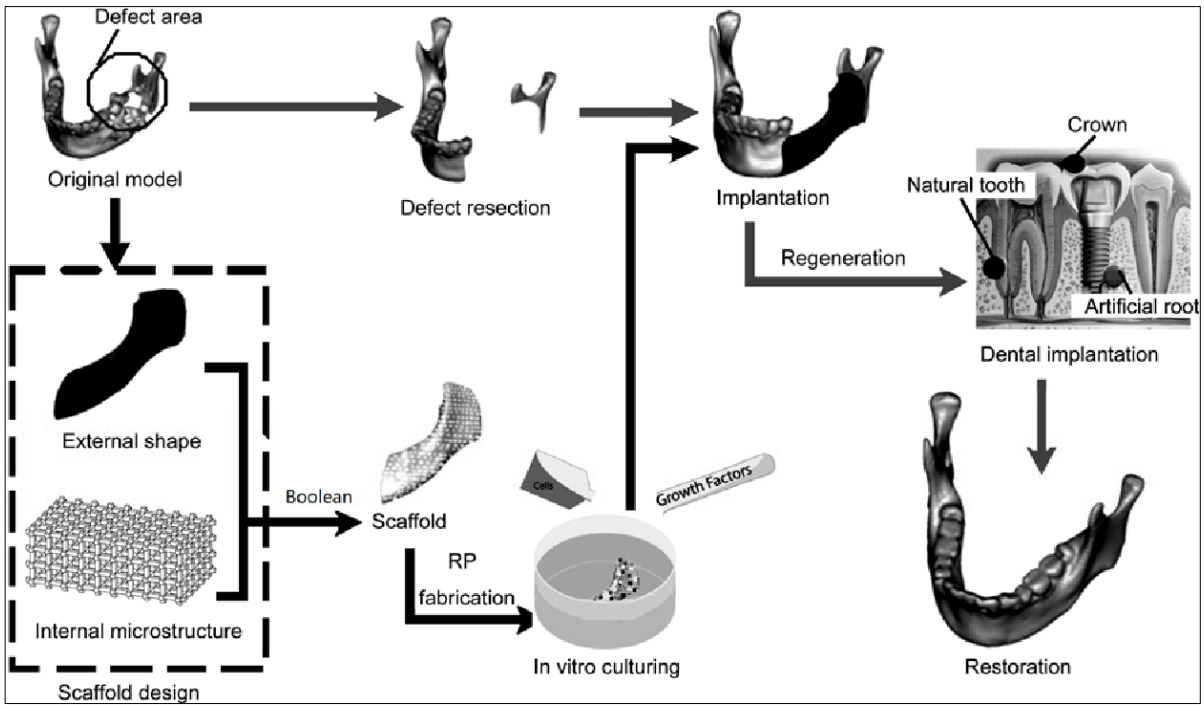

Figure 2.9. Mandible repaired by scaffold tissue engineering [11].

2.4.5.1 3D Scaffolds

Using synthetic scaffolds enables us to design and control the replacement implant size and mechanical properties to fit the host bone requirements. Bone can be grown in the defective site without failure risks (figure 2.9) [11]. This material has an assistive role in tissue growth factors and accelerates bone healing for cases where the defect size is big enough to prevent the reunion of separated segments. As previously discussed, scaffolds are porous structures that can cause cell proliferation and differentiation within their microchannels. On the other hand, they control the biomechanic forces properly so that the damaged part does not experience extra stress. They also form the primary form of damaged bone [51,52].

Fluid flow dynamics in porous scaffolds play an important role in tissue engineering for transferring essential materials to cells and controlling the biocompatibility of scaffolds. Properties such as permeability and wall shear stress due to fluid flow determine the biological behavior of scaffolds. Bioactivity depends on the release of oxygen and other nutrients through the porous medium, and shear stress due to fluid flow is recognized as the dominant mechanical stimulus for cell differentiation and proliferation in scaffolds [12].

2.4.5.2 Scaffolds Materials and Fabrication Methods

Scaffolds for bone tissue replacement are mainly made from metal, ceramics, and polymers or their composites. The techniques can be divided into conventional and advanced scaffolds fabrication methods. The traditional techniques include solvent casting particulate leaching, melt molding, gas foaming, and freeze-drying processes. However, advanced methods such as electrospinning and 3D printing have been developed recently [1, 52, 53].

Ceramic Scaffolds

Hydroxyapatite, calcium phosphates, or composites made of them are ceramics that show the closest properties to bone tissue because they contain bioactive elements. These materials illustrate effective biological interactions with bone, facilitating fusion with bone tissue and fixation of bone to the scaffold. Moreover, silicate bioactive glasses such as 45S5 Bioglas® can promote rapid bone formation by releasing critical amounts of ions such as Si, Ca, P and Na [54]. This type of scaffold can be manufactured using gel casting or robocasting methods. In the gel-casting technique, scaffolds with an amorphous morphology are obtained, and in the robocasting process, scaffolds with relatively regular architecture can be produced [55].

Metal Scaffolds

Metals like titanium (Ti) (and its alloys), 316 L stainless steel, and magnesium are widely used for bone implants and scaffolds. Due to their high mechanical properties,

biocompatibility, and exceptional corrosion resistance, these metals show promising results in producing scaffolds for bone. However, disadvantages like poor bone induction ability and high modulus of elasticity relative to the host bone should be considered for these types of scaffolds [56].

Recently, magnesium has been considered a scaffold material for bone healing due to its good mechanical resistance and biodegradability. Nevertheless, challenges such as controlling the degradation time and rate, also, the non-compliance of its mechanical properties with the host bone remain unsolved [57].

Polymer Materials Scaffolds

Polyglycolic acid (PGA), polylactic acid (PLA), and its copolymers, and polylactic co-glycolic acid (PLGA) are the most well-known and familiar polymers that are widely used for bone replacement applications. For example, PLA is a bio-degradable material that is easy and cheap to produce with 3D printers. The obtained structure has pores of 0,3 mm, which is very close to human bone pore size [58].

2.5 ART OF BONE SCAFFOLD DESIGN

Bone is a tissue that can rebuild its defects in conditions when separated bones can send signals to each other. This process can take weeks or months for many bone fractures without external operation [59, 60]. But, when a major segmental bone defect is above a crucial size (roughly 8 mm), the body typically cannot complete the healing [61]. Therefore, that empty place needs an external intervention to help the healing and rebuilding process in the defected site [64].

In tissue engineering, the distribution and delivery of essential materials to bone cells and the management of the scaffold's biocompatibility depend on fluid flow dynamics inside the porous scaffold. For this reason, we need porous material that can provide a suitable environment for cell profiliation and differentiation. Designing scaffolds with such permeability and suitable mechanical properties to withstand biomechanical loads is challenging for tissue engineers [62].

Researchers have tried to produce scaffolds for bone with quite different architectures. These two scaffold groups achieve higher porosity rates that meet bone healing requirements. The first is group lattice scaffolds and consists of thin rods connected at the ends. The other group of scaffolds is defined as Triply Periodic Minimal Surfaces. As surfaces with a thin wall thickness, these scaffolds are repeated in the direction of the three axes of the coordinate system to form the scaffold structure in the desired dimensions (Figure 2.10) [63].

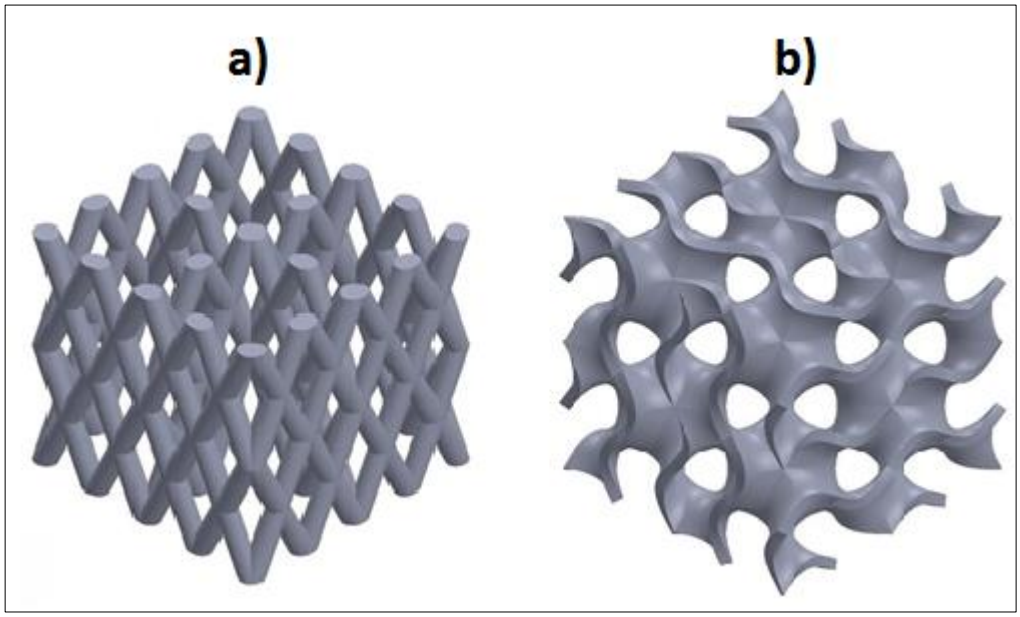

Figure 2.10. Tow typical scaffolds for bone tissue engineering; a) Lattice-based and b) TPMS scaffolds [63].

These two groups of scaffolds have been investigated in terms of their biological and mechanical behavior. However, only a few studies investigated their performance under actual biomechanical loading conditions to the authors' best knowledge. To overcome such a gap, in this work, four different scaffolds with lattice structures were studied to test their performance in a mandible bone defect under biomechanical loads. For the first group, simplicity of design and production can be considered an advantage. For the second group, the high ratio of surface to volume is an essential parameter in the biocompatibility of scaffolds is regarded as a preponderance.

CHAPTER 3

METHODOLOGY

3.1 MATERIALS

3.1.1 MANDIBLE BONE AND CAD MODELS

In this study, the mandible bone 3D model was obtained using computed tomography using Dassault Systèmes SOLIDWORKS (2017) software, the cortical segment use designed with a fixed thickness of 1.8 mm [11] separated from cancellous bone section and a cube defect with the size of 8.57×8.57×8.57 mm^3 in symphysis site and the designed scaffolds were replaced the defect. (Figure 3.1).

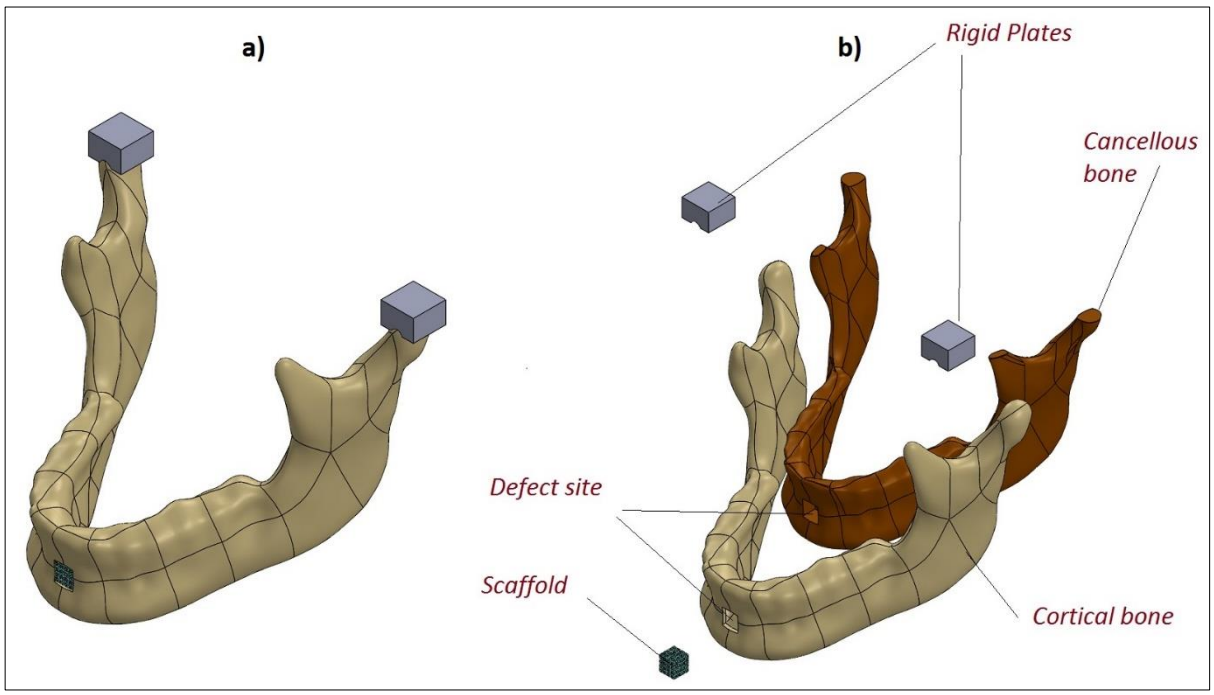

Figure 3.1. a) CAD model and its b) exploded view of the parts.

3.1.2 SCAFFOLD MODELS

In this study, the designed scaffolds are in the different architecture of scaffolds namely as Octet [64], Octahedron [65], Cubic Body Center [66] and, Rhombicuboctahedron [67] with a porosity of 80%. The CAD model of scaffolds was obtained by repeating 4x4x4 along the x, y, and z-axis using their unit cells (Figure 3.2). A fixed unit cell size for all the scaffold models the rod diameter for Octet, Octahedron, Cubic body center, and Rhombicuboctahedron was 300, 440, 390, and 340 µm, respectively.

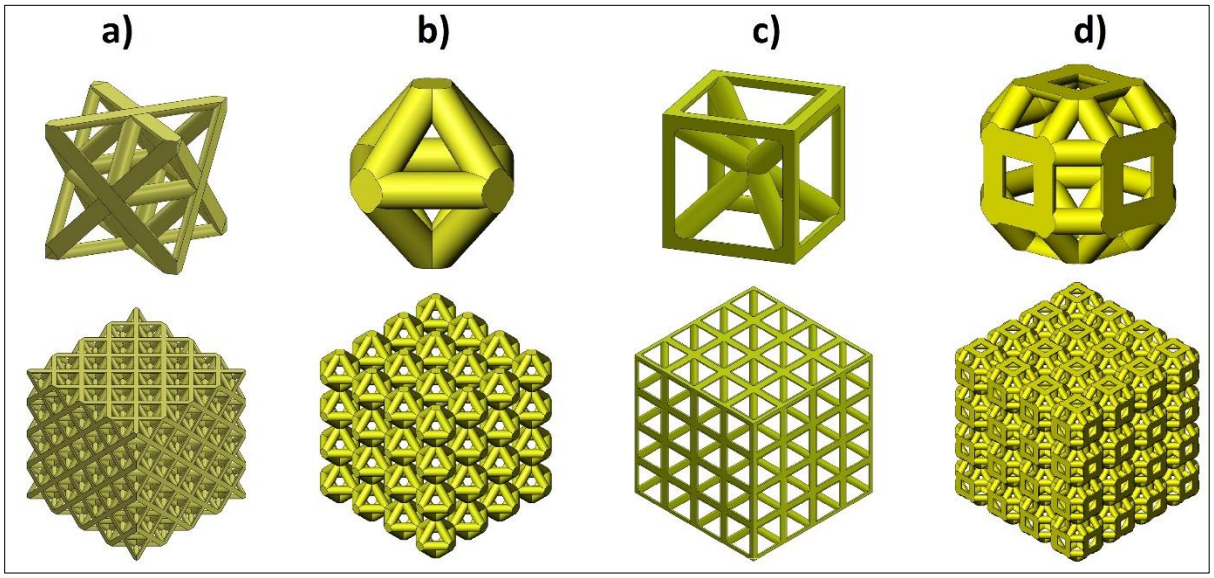

Figure 3.2. CAD models of the scaffolds and their unitcells; a) Octet 300 µm , b) Octahedron 440 µm , c) Cubic Body Center 390 µm and d) Rhombicuboctahedron 340 µm.

3.1.3 Finite Element Analysis (FEA)

Designed scaffolds in Dassault Systèmes SOLIDWORKS (2017) were sent to ANSYS Workbench (18) to calculate the stress distribution on bone-scaffold contact surfaces. The analysis was performed in the elastic region of the material. Also, the material was assumed as isotropic and homogeneous. In this study for the cortical and cancellous bones, a constant elastic modulus was assigned. For the scaffolds, three different material elasticity was applied (Table 3.1). Therefore, a total amount of twelve FEA

models were tested. The contact between all the parts was considered as fully bonded surfaces [68].

Table 3.1**.** Material properties for the FEA models.

Material	**Young's Modulus (GPa)**	**Poisson's Ratio v**
Cortical Bone	15 [69]	0.3
Cancellous bone	1.5 [70]	0.33
Ti6A14V Scaffold	110 [71]	0.3
Mg Scaffold	30 [72]	0.3
Polymeric Scaffold (PLA)	4 [71]	0.34
Rigid body	1200 [50]	0.3

3.1.4 Meshing The Models

The FEA models were mesh using tetrahedral elements [73]. A maximum element size of 0.9 mm for the whole of the models was selected. To ensure mesh independence of the FEA results a very fine mesh was selected in defect and scaffold surface area (Figure 3.3).

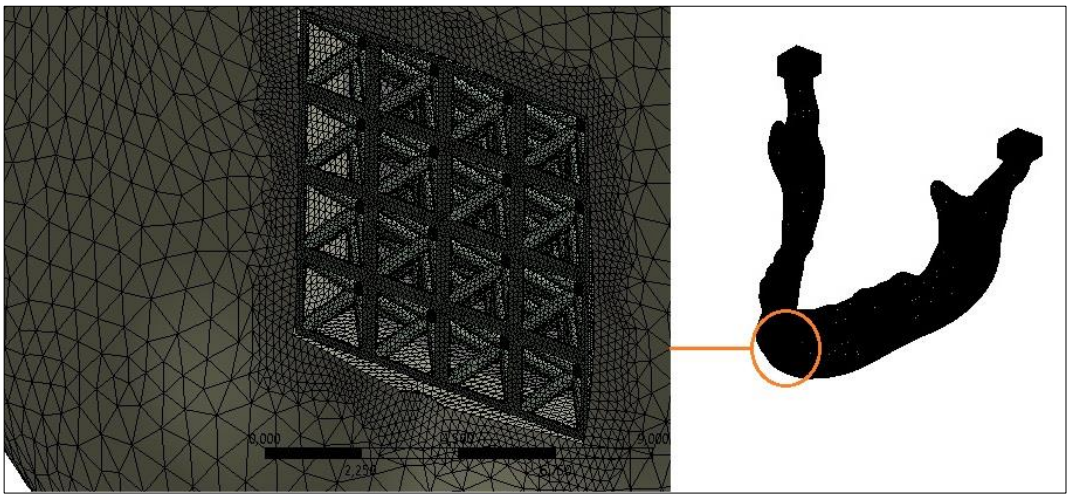

Figure 3.3. Whole model mesh and refined mesh in the scaffold-bone contact area.

The mesh statistics for each model are presented in table 3.2. Because of scaffolds architecture difference in this study, the mesh number for each model is different.

Table 3.2. Mesh statistics of FEA models

Scaffold model	**Octet**	**Octahedron**	**Cubic Body Center (CBC)**	**Rhom Bicuboctahedron (T)**
Element Number	1876483	1883856	1884515	1910998

3.1.5 Boundary Condition

The biting and muscle forces direction and magnitude are shown the figure 3.4 and table 3.3. Also, the models are fixed from the condyle site on both sides (figure 3.4) [74].

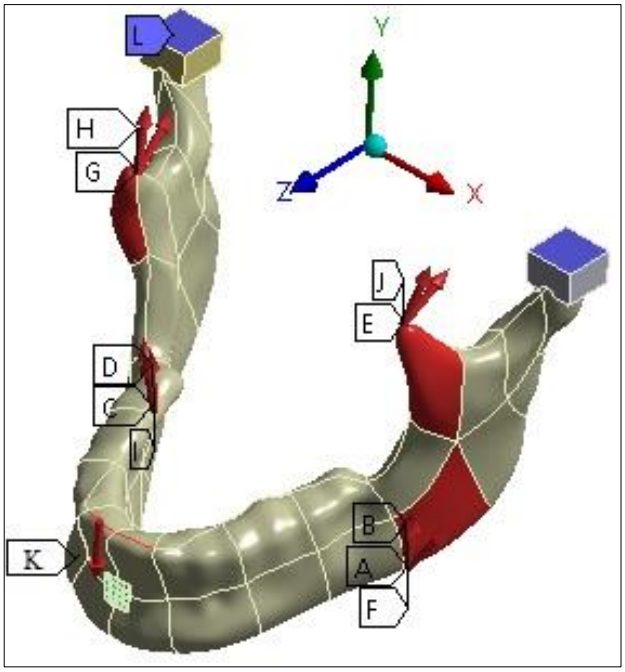

Figure 3.4. The muscle force and bite force in the FEA model.

Table 3.3**.** The applied muscle and bite forces (N) in FEA [75].

Force	Ref.	X	Y	Z
Deep Massester	A,B	7.776	127.23	22.68
Superficial Masseter	D,C	12.873	183.5	12.11
Medical Pterygoid	F,I	140.38	237.8	-77.3
Temporalis	E,G	0.0064	0.37	-0.13
Medial Temporal	H,J	0.97	5.68	-7.44
Bitting Force	K		100	

3.1.6 Eq. von Mises STRESS

The von Mises criterion is adapted from Richard von Mises's German-American mathematician (1883-1953). The von-Mises stress criterion (Collision energy theory or strain energy theory) is based on the distortion energy in a given material. According to this criterion, deterioration occurs when the amount of energy accumulated in a particular fabric reaches the energy level at which the same material will flow under tension or pressure. In other words, as long as the energy collected under external loads in any part remains under the distortion energy per unit volume required to produce yielding in the tensile-test sample of the same material, that part is in a safe condition for use. In this numerical study, to understand the distribution of stress in the contact region, only von Mises' stress was calculated (Equation 3.1). The distortion energy per unit volume of isotropic material under tension can be written as [76]:

$$\sigma_{vm} = \sqrt{0.5\left[\left(\sigma_x - \sigma_y\right)^2 + \left(\sigma_y - \sigma_z\right)^2 + (\sigma_z - \sigma_x)^2\right] + 3\left[\tau_{xy}^2 + \tau_{xz}^2 + \tau_{yz}^2\right]} \quad (3.1)$$

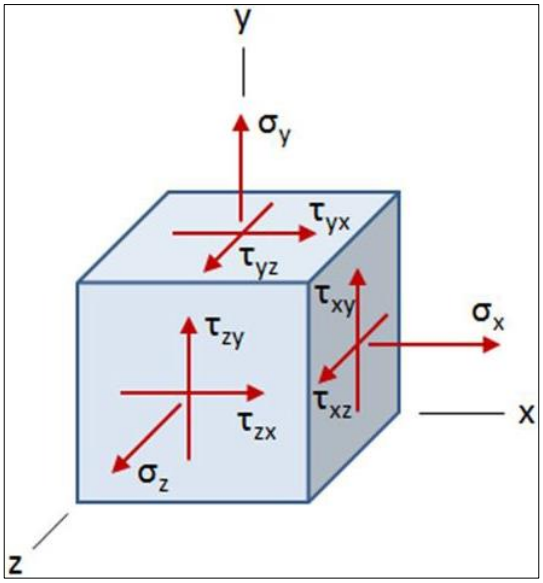

Figure 3.5. Stress Tensor Element.

CHAPTER 4
RESULTS AND DISCUSSION

4.1 RESULTS RELIABILITY

To test the FEA result reliability the total deformation of models under the applied boundary condition was measured (Figure 4.1).

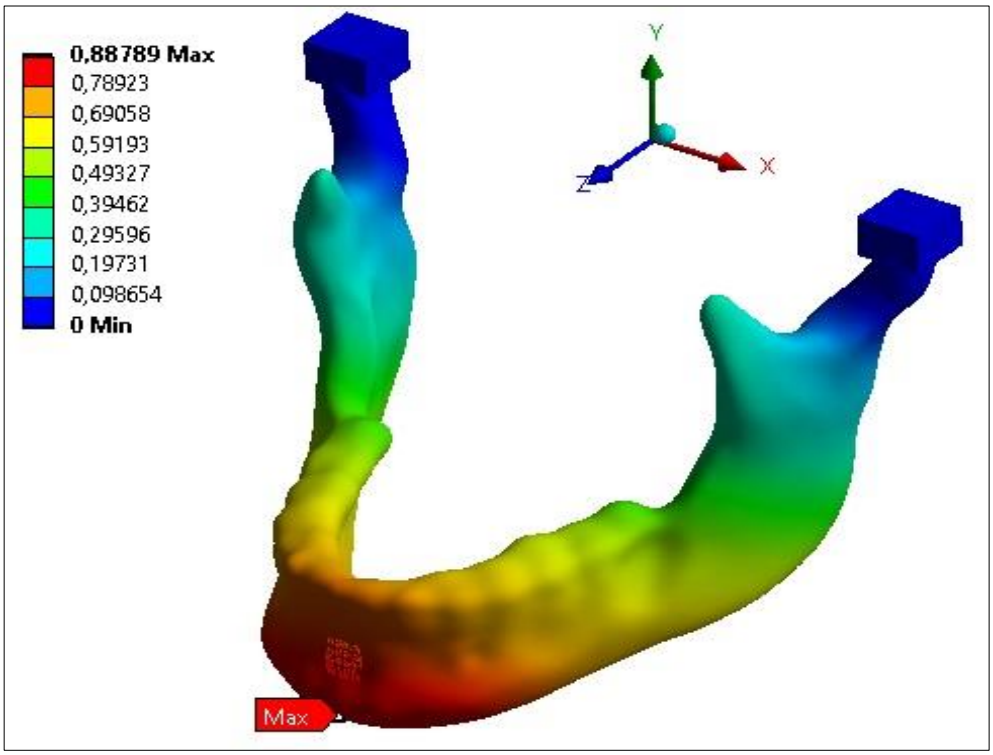

Figure 4.1. The total deformation of the mandible under the muscles and bite force.

The total deformation for all the models approximately was the same for such muscles and bite force, and this magnitude is inconsistent with similar works result in the literature [77,78].

4.2. VON MISES STRESS IN SCAFFOLDS

To elucidate the behavior of scaffolds under such biomechanical loading, the von Mises stress of them was calculated. For example, the von Mises stress for Rhombicuboctahedron-Ti was demonstrated in figure 4.2.

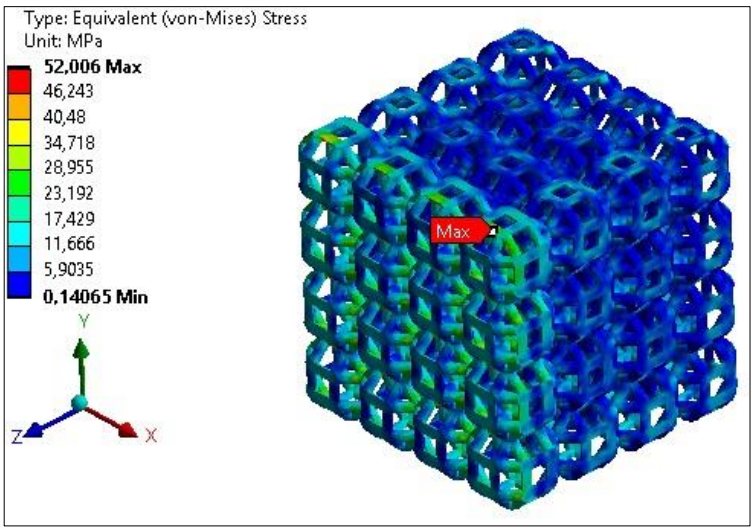

Figure 4.2. Von Mises stress contour in Rhombicuboctahedron-Ti n scaffold.

Maximum equallent von Mises stress (max eq. vM. S) for each model was presented in figure 4.3.

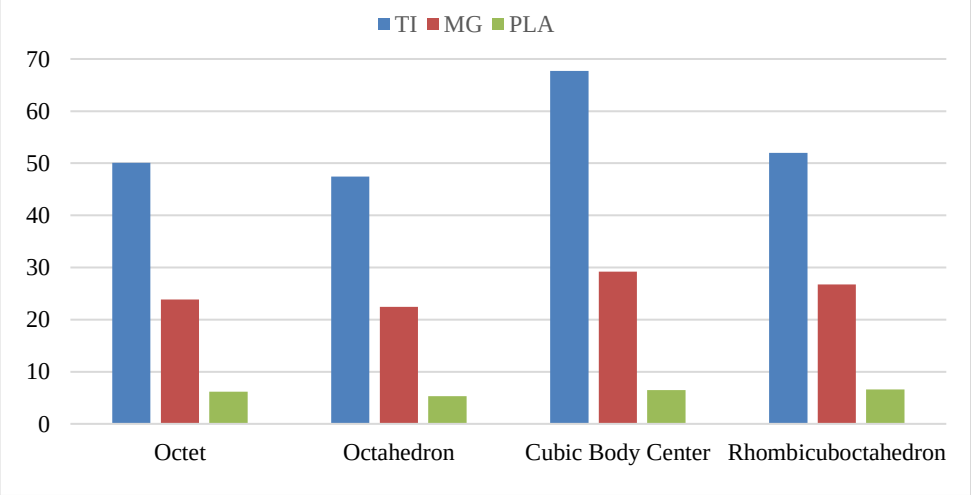

Figure 4.3. The calculated max. vM. s (MPa) in the scaffolds.

The highest and lowest von Mises stresses were seen for the Ti and polymer-based models, respectively, in all four scaffolds with the same architecture, and the mg-based models were positioned in the middle of these two. In terms of architectural effect, the CBC models showed the highest maximum von Mises stress, and the other three models behaved very similarly. According to the results in figure 4.3, among all the models the scaffolds with octahedron architecture and PLA material showed the lowest von Mises stress.

4.3. EQ. VM. S ON CANCELLOUS BONE CONTACT SURFACE WITH SCAFFOLD

Compared to cortical bone, cancellous bone possesses low mechanical properties, and any stress concentration on it can lead to undesirable consequences. The vM. stress on the contact surface between cancellous bone and scaffold for all the models were calculated. For example, the vM.s distribution for the Rhombicuboctahedron Ti model was demonstrated in figure 4.4.

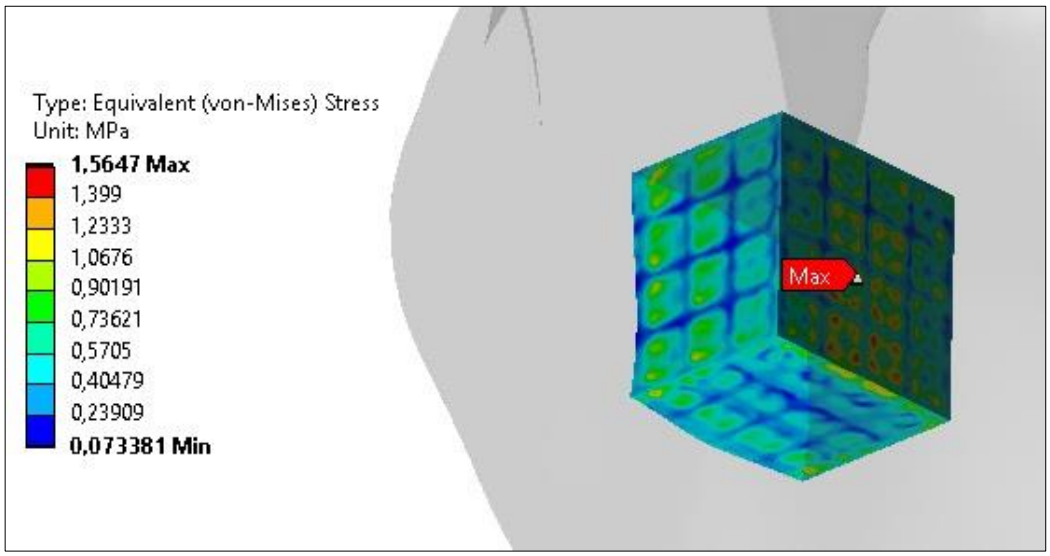

Figure 4.4. vM.s distribution in cancellous bone contact surface in Rhombicuboctahedron-Ti model.

To show the effect of scaffold architecture, as well as the assigned material stiffness on the contact region, stress the maximum von Miss stress for all models, was presented in figure 4.5.

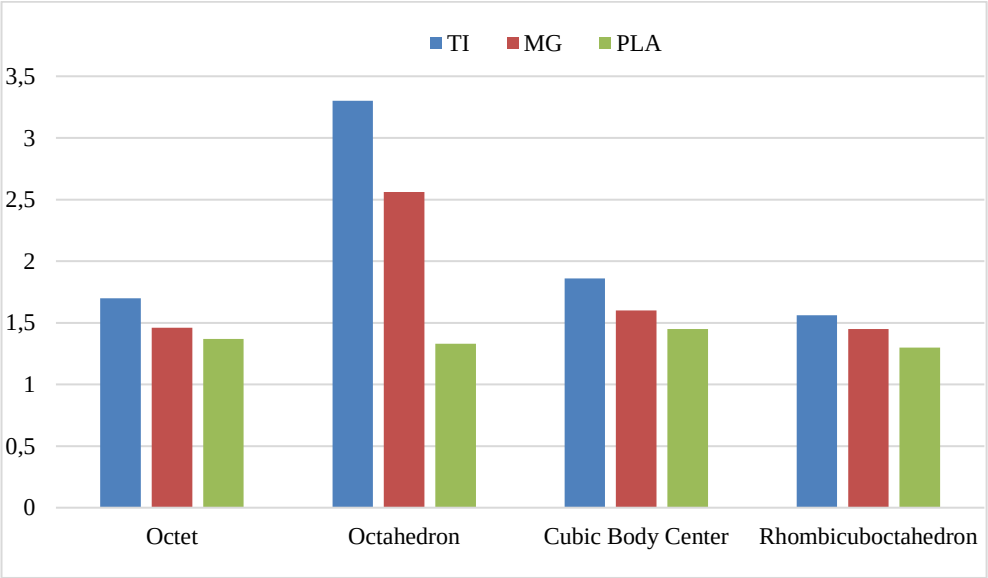

Figure 4.5. The max. vM. s (MPa) in cancellous bone contact surface with scaffold.

As can be seen, the maximum vM.s obtained on the surfaces varies with the scaffold architecture and assigned material. In all the four architecture groups, the highest vM.s belong to Ti scaffold models and the lowest emerged in models with PLA selected material. From an architectural point of view, the greatest effect of changing the scaffold material on stress can be seen for the octahedron model, so that by changing the scaffold material from Ti to PLA, the vM.s was reduced by half. In general, with decreasing scaffold stiffness, stress at cancellous bone contact surfaces reduced for all the models.

4.4. vM.S ON CORTICAL BONE CONTACT SURFACE WITH SCAFFOLD

Although compared to cancellous the cortical bone is a stronger material, stress accumulation can damage its structure and can delay the healing process. Therefore, in scaffold implantation, it should be given enough attention to avoid such undesirable situations. To probe stress distribution on the cortical bone surface, for example, the

vM.S contour for Rhombicuboctahedron-Ti was demonstrated in figure 4.6. The vM.s fluctuated between 0.2- 6.82 MPa on the contact region for such a model.

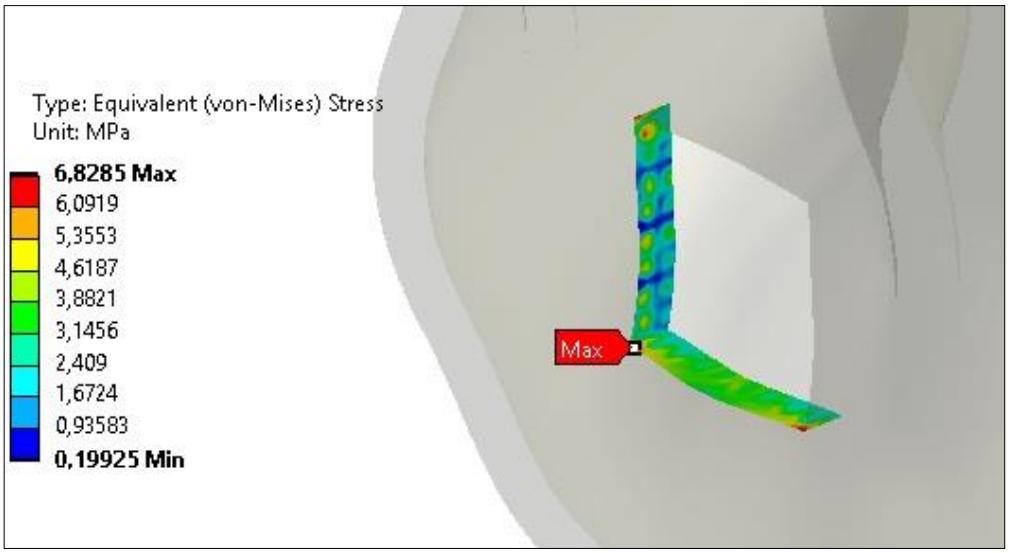

Figure 4.6. vM.s contour in cortical bone and scaffold contact area for the Rhombicuboctahedron-Ti model.

Also, to observe the effect of architecture and scaffolding material on the stress of the contact surfaces, the maximum stress for all models was shown in figure 4.7.

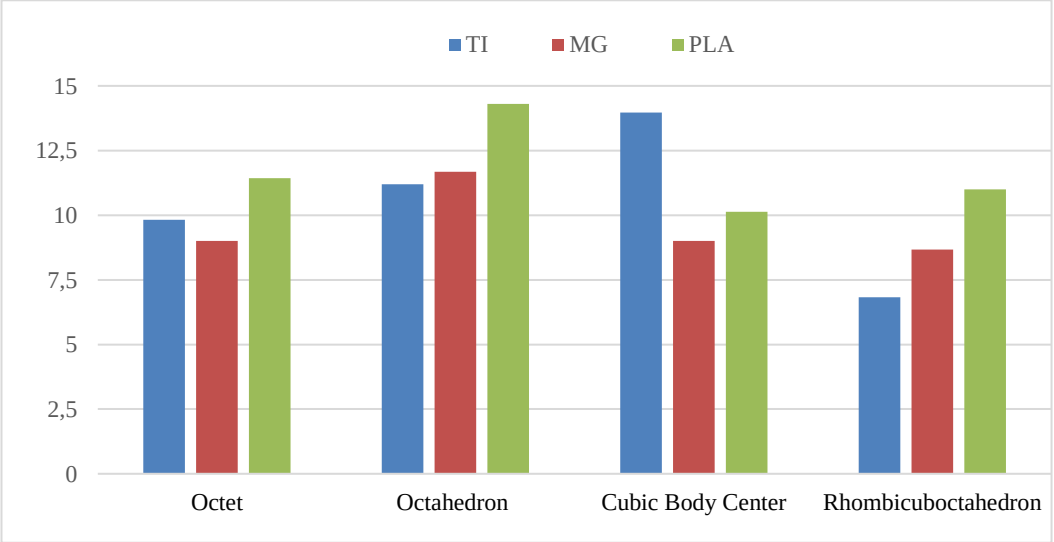

Figure 4.7.The max. vM. s on the cortical bone contact surface with scaffold for all the models.

For the models with octahedron and Rhombicuboctahedron a decreased scaffold stiffness the maximum vM.s stress increased. For two other groups (Octet and CBC) of the scaffold, such a trend cannot be seen. In other words, for the recent two groups, the maximum vM.s first decreases with changing the material from Ti to Mg, but after changing it to PLA, we observe a jumping in maximum vM.s value. Therefore, at least for scaffolds with octahedron and CBC architecture, finding a predictable stress attitude versus material rigidity is difficult.

4.2 DISCUSSION

Indeed, stress shielding eraises from the mismatch in stiffness between scaffolds and host bone that causes an undesirable load transfer between surfaces in implanting sites [79]. Therefore, designing and finding scaffolds that can proportionately transmit biomechanical forces is challenging for tissue engineers. In scaffolds, the stiffness is a function of architecture and selected material [80,81]. Because experimental studies are expensive and time-consuming, engineers use computer simulations to obtain mechanically optimized scaffolds to minimize side effects like stress concentration. This study modeled four scaffolds with different architectures to replace a mandible bone defect. We also studied the effect of materials selected for scaffolds on stress shielding using three different materials. Before dealing with the accumulation of stress at the contact surfaces, it would be better to examine the magnitude of stress that happend in the scaffold's structure to make sure that the scaffold remains in the elastic region under such loading conditions. Therefore, examining the stress map in the scaffold helps us determine whether the scaffold can withstand such loads. For example, the eq.vM.s for four different scaffold architecture with Ti alloy material was illustrated in figure 4.8. As seen, the maximum stress up to 42% can vary by changing the architecture of the scaffold. Although the max.eq.vM.s for all four scaffolds occurred in the area of contact with the cortical bone, it should be noted that its point is located entirely in different unit-cell for all of them. It can be concluded that the max.eq.vM.s zone is the same for all the models, but its exact location varies from a scaffold to scaffold.

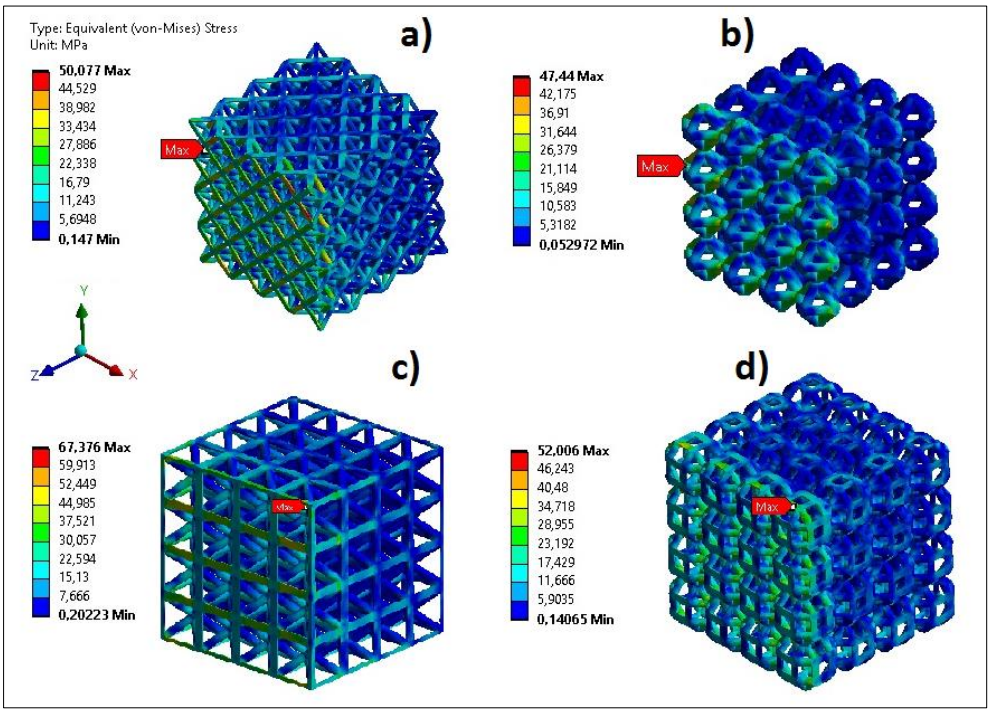

Figure 4.8. vM.s contour for scaffolds with Ti alloy material. a) Octet, b) Octahedron, c) Cubic body center, and d) Rhombicuboctahedron.

For a titanium specimen made by selective laser melting, which is the predominant method in manufacturing metal scaffolds, a yield strength of about 1000 MPa is reported [13]. Therefore, we can be sure that the resulting vM.s stress on the scaffolds will not cause yield. We can also extend this to this study's magnesium and polymer-based scaffolds. The yield strengths of magnesium and polymer are reported to be about 200 and 50 MPa [79,80], respectively, and figure 4.8 shows that the max.eq.vM.s are still below such magnitudes in the last two scaffold groups. It can be concluded that in this study, all the scaffold models will remain in the elastic zone. Therefore, at least for the load used in this study, the scaffolds material does not determine whether it yields or not.

Let's further discuss the stress on the contact surfaces of the cancellous bone, which is weaker than the cortical bone, and the possibility of damage at the contact region with the scaffold is relatively high. Figure 4.8 showed us that the highest vM.s stress occurred in models with titanium scaffold. Therefore, the vM.s contour for the above

models is shown in figure 4.9. to understand stress distribution modality through the contact surfaces.

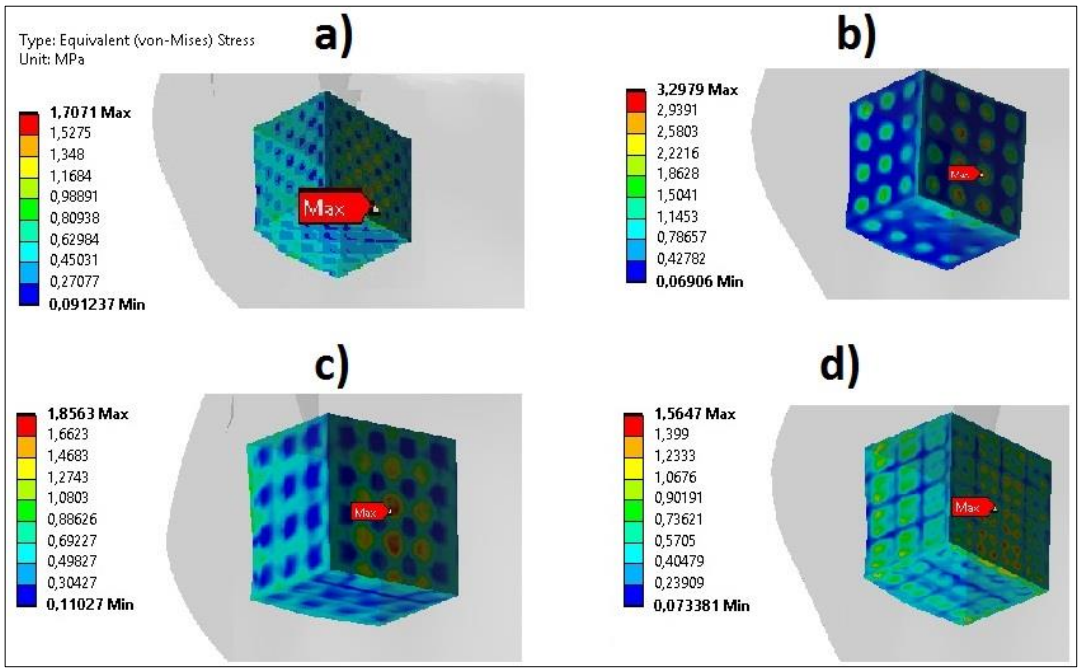

Figure 4.9. vM.s contour on cancellous bone contact surface for the models with Ti alloy scaffolds. a) Octet, b) Octahedron, c) Cubic body center, and d) Rhombicuboctahedron.

As shown in figure 4.9, the stress changes from one model to another can be doubled. And this shows the importance of choosing a proper scaffold architecture for such orthopedic applications. According to the results given in Figure 4.9 and also the yield stress of 3.5 MPa for the cancellous bone [81], it is quite clear that at least under the loading modeled in this study, the cancellous bone will remain undamaged.

Although the cortical bone is relatively strong, it has a thin thickness in the mandible that may lose its endurance if stress concentrates in it. Therefore, it is necessary to discuss the distribution of stress on the cortical bone and scaffolds contagt regions.

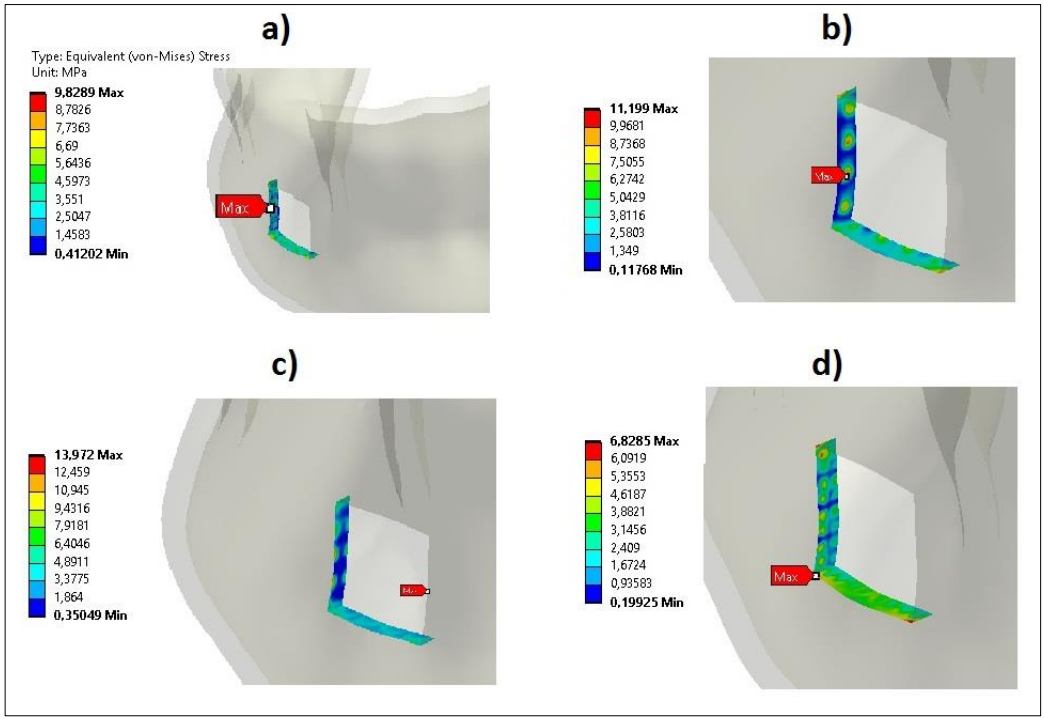

Figure 4.10. vM.s contour on cortical bone contact surface for the models with Ti alloy scaffolds. a) Octet, b) Octahedron, c) Cubic body center body center and d) Rhombicuboctahedron.

Figure 4.10 shows the distribution of vM.s in the contact area of the scaffold with the cortical bone. According to the vM.s contour, its maximum value can be up to twice in one model compared to another. This is a reaffirmation of the importance and role of scaffolds architecture in transferring load in orthopedic implantation using scaffold structures. Unlike the above two cases (vM.s on scaffolds and cancellous bone surfaces), figure 4.9 shows almost no significant relationship between scaffolding material and the amount of stress calculated on the surface of cortical bone. It isn't easy to find a logical explanation for such a result. Still, it can be said that because the scaffold is in contact through a smaller area in cortical bone compared to cancellous bone the biomechanical force caused the greater stress.

The scaffolds being contacted to the mandible bone from five faces (Figure 3.1) worths nothing significant. The contact surface area for scaffolds octet, octahedron, cubic body center, and Rhombicuboctahedron is 126.85, 16.02, 121.35, and 101 is 126.85, 16.02, 121.35 and 101 mm^2, respectively. As can be seen, the octahedron scaffold has the lowest contact surface area. Relative higher vM.s in the cancellous bone surface

containing this scaffold (figure 4.4) can be justified. But the influence of sharpness of scaffolds corners can also be a parameter that should be investigated in future studies.

CHAPTER 5

SUMMARY

This theoretical study investigated the force transmission modality between the scaffold and the host bone with computer simulation. We used four different scaffold architectures that are widely used in the literature. The results of this work can be summarized as follows:

- To the authors' best knowledge, this is the first numerical study to analyze the effect of scaffolds architecture and material on stress distribution within contact region at a defected mandible bone, which shed more light on the design and chose suitable scaffolds for similar clinical applications.

- The magnitude of the stress in the scaffold's structure was more related to its material than its architecture. There was less stress on the scaffolds and cancellous bone surface with softer scaffolds. Minor stress for such scaffolds doesn't mean anything because the success of a scaffold depends on other parameters such as fatigue failures. Therefore, investigating the effect of fatigue stress during bone treatment requires more experimental and theoretical studies.

- The calculated stresses in cancellous bone and scaffolding did not show a significant relationship with the type of scaffolds architecture. However, in terms of stress shielding in cancellous bone, the scaffold with Rhombicuboctahedron architecture caused less stress than the other three in cancellous bone and had better performance.

- For the calculated stresses on the cortical bone, almost neither of the two architectural parameters of the material and the scaffold showed a trend. This can be explained by the low contact surface of the scaffold with that bone compared to

the spongy bone. It seems that in this bone, the magnitude of stress that happens at the surfaces in contact with the scaffold is determined by other parameters such as the sharpness of the scaffold.

- With all limitations of this study, it is inferred from the results that the force transmission conditions in the scaffold contact area with the host bone depend on a combination of factors. Future studies should examine all these parameters where stress shielding is an undesired phenomenon in implantation.

REFERENCES

1. Win Naing, M., Chua, K., Leong, K. F., and Wang, Y., "Fabrication of customised scaffolds using computer-aided design and rapid prototyping techniques", ***Rapid Prototyping Journal***, 11: 249–259 (2005).

2. Shek, F. W. and Benyon, R. C., "How can transforming growth factor beta be targeted usefully to combat liver fibrosis?", ***European Journal Of Gastroenterology & Hepatology***, 16 (2): 123–126 (2004).

3. Silva, M., Cyster, L., Barry, J., Yang, X., Oreffo, R., Grant, D., Scotchford, C., Howdle, S., Shakesheff, K., and Rose, F., "The effect of anisotropic architecture on cell and tissue infiltration into tissue engineering scaffolds", ***Elsevier,*** 27 (35): 5909–5917 (2006).

4. Bose, S., Roy, M., and Bandyopadhyay, A., "Recent advances in bone tissue engineering scaffolds", ***Trends In Biotechnology***, 30 (10): 546–554 (2012).

5. "Biomaterials & Scaffolds for Tissue Engineering - ScienceDirect", **https://www.sciencedirect.com/science/article/pii/S136970211170058X** (2022).

6. Kayumi, S., Takayama, Y., Yokoyama, A., and Ueda, N., "Effect of bite force in occlusal adjustment of dental implants on the distribution of occlusal pressure: comparison among three bite forces in occlusal adjustment", ***International Journal Of Implant Dentistry***, 1 (1): 14 (2015).

7. Shahi, A. K., Prajapati, V. K., Shandilya, V., and Singh, R. K., "Bony Healing Following Filling of Post Cystectomy Jaw Bone Defects with Hydroxyapatite and Beta-Tricalcium Phosphate and its Comparison with Non-Filling Case: A Clinical Study", ***International Journal Of Scientific Study***, 3 (9): 102–106 (2015).

8. Yan, C., Hao, L., Hussein, A., and Young, P., "Ti–6Al–4V triply periodic minimal surface structures for bone implants fabricated via selective laser melting", ***Journal Of The Mechanical Behavior Of Biomedical Materials***, 51: 61–73 (2015).

9. Malheiro, V. N., Spear, R. L., Brooks, R. A., and Markaki, A. E., "Osteoblast and monocyte responses to 444 ferritic stainless steel intended for a magneto-mechanically actuated fibrous scaffold", ***Biomaterials***, 32 (29): 6883–6892 (2011).

10. Luo, D., Rong, Q., and Chen, Q., "Finite-element design and optimization of a three-dimensional tetrahedral porous titanium scaffold for the reconstruction of mandibular defects", ***Medical Engineering & Physics***, 47: 176–183 (2017).

11. Liu, Y., Zhu, F., Dong, X., and Peng, W., "Digital design of scaffold for mandibular defect repair based on tissue engineering", ***Journal Of Zhejiang University SCIENCE B***, 12 (9): 769 (2011).

12. Pasha Mahammod, B., Barua, E., Deoghare, A. B., and Pandey, K. M., "Permeability quantification of porous polymer scaffold for bone tissue engineering", ***Materials Today: Proceedings***, 22: 1687–1693 (2020).

13. Parthasarathy, J., Starly, B., Raman, S., and Christensen, A., "Mechanical evaluation of porous titanium (Ti6Al4V) structures with electron beam melting (EBM)", ***Journal Of The Mechanical Behavior Of Biomedical Materials***, 3 (3): 249–259 (2010).

14. Zhang, L., Song, B., Choi, S.-K., and Shi, Y., "A topology strategy to reduce stress shielding of additively manufactured porous metallic biomaterials", ***International Journal Of Mechanical Sciences***, 197: 106331 (2021).

15. Yang, Y., Wang, G., Liang, H., Gao, C., Peng, S., Shen, L., and Shuai, C., "Additive manufacturing of bone scaffolds", ***International Journal of Bioprinting***, 5 (1): (2019).

16. Wong, C., Loh, J. S., and Islam, I. P. F. Elem. M., "The Role of Finite Element Analysis in Studying Potential Failure of Mandibular Reconstruction Methods", ***Perusal Finite Elem. Method***, 189–210 (2016).

17. Wong, R., Tideman, H., Kin, L., Merkx, M. J I. journal of oral, and surgery, maxillofacial, "Biomechanics of mandibular reconstruction: a review", ***International journal of oral and maxillofacial surgery,*** 39 (4): 313–319 (2010).

18. Weijs, W. and Hillen, B. J J. of D. R., "Relationships between masticatory muscle cross-section and skull shape", ***Journal of Dental Research,*** 63 (9): 1154–1157 (1984).

19. Xie, S. S., "Physiological Model of the Masticatory System", Advanced Robotics for Medical Rehabilitation, ***Springer***, 45–79 (2016).

20. Chim, H., Salgado, C. J., Mardini, S., and Chen, H.-C., "Reconstruction of mandibular defects", ***Seminars in Plastic Surgery***, (2010).

21. Kumar, B. P., Venkatesh, V., Kumar, K. J., Yadav, B. Y., Mohan, S. R. J J. of maxillofacial, and surgery, oral, "Mandibular reconstruction: overview", ***Maxillofacial Plastic and Reconstructive Surgery,*** 15 (4): 425–441 (2016).

22. Yemineni, B. C., Maiti, S., Datta, A., Ali, S. V., Singh, V., Thakur, D., and Jain, R. H., "Various Modalities of Mandibular Defects Reconstruction: Overview", ***Saudi Journal of Medicine*** ,(2020).

23. Miller, C. P., Chiodo, C. P. J F., and Clinics, A., "Autologous bone graft in foot and ankle surgery", ***Foot and ankle clinics***, 21 (4): 825–837 (2016).

24. IVY, R. H. J P. and Surgery, R., "Bone grafting for restoration of defects of the mandible", ***Plastic and Reconstructive Surgery,*** 7 (4): 333–341 (1951).

25. Tessier, P., Kawamoto, H., Matthews, D., Posnick, J., Raulo, Y., Tulasne, J. F., Wolfe, S. A. J P., and surgery, reconstructive, "Taking long rib grafts for facial

reconstruction–tools and techniques: III. A 2900-case experience in maxillofacial and craniofacial surgery", ***Plastic and reconstructive surgery,*** 116 (5): 38S-46S (2005).

26. White, S. J B. medical journal, "The employment of silver wire to bridge the gap after resection of a portion of the lower jaw", ***British medical journal***, 2 (2552): 1525 (1909).

27. Attie, J., Catania, A., and Ripstein, C. J S., "A stainless steel mesh prosthesis for immediate replacement of the hemimandible", ***Surgery,*** 33 (5): 712–720 (1953).

28. Blocker Jr, T., STOUT, R. A. J P., and Surgery, R., "Mandibular reconstruction, World War II", ***Plastic and Reconstructive Surgery***, 4 (2): 153–156 (1949).

29. Wersäll, J., Bergstedt, H., Körlof, B., Lind, M. G. J O., and Surgery, N., "Split-rib graft for reconstruction of the mandible", ***Otolaryngology—Head and Neck Surgery***, 92 (3): 270–276 (1984).

30. Swartz, W. M., Banis, J. C., Newton, E. D., Ramasastry, S. S., Jones, N. F., Acland, R. J P., and surgery, reconstructive, "The osteocutaneous scapular flap for mandibular and maxillary reconstruction", ***Plastic and reconstructive surgery,*** 77 (4): 530–545 (1986).

31. Hidalgo, D. A. J P. and surgery, reconstructive, "Fibula free flap: a new method of mandible reconstruction", ***Plastic and reconstructive surgery,*** 84 (1): 71–79 (1989).

32. Liu, H. and Webster, T. J., "Bioinspired nanocomposites for orthopedic applications", Nanotechnology for the Regeneration of Hard and Soft Tissues, ***World Scientific***,1–51 (2007).

33. Jewer, D. D., Boyd, J. B., Manktelow, R. T., Zuker, R. M., Rosen, I. B., Gullane, P., Rotstein, L. E., Freeman, J. E. J P., and surgery, reconstructive, "Orofacial and mandibular reconstruction with the iliac crest free flap: a review of 60 cases and a new method of classification", ***Plastic and reconstructive surgery***, 84 (3): 391–403; discussion 404 (1989).

34. Maurer, P., Eckert, A. W., Kriwalsky, M. S., Schubert, J. %J B. J. of O., and Surgery, M., "Scope and limitations of methods of mandibular reconstruction: a long-term follow-up", ***British Journal of Oral and Maxillofacial Surgery,*** 48 (2): 100–104 (2010).

35. Warren, S. M., Borud, L. J., Brecht, L. E., Longaker, M. T., Siebert, J. W. %J P., and surgery, reconstructive, "Microvascular reconstruction of the pediatric mandible", ***Plastic and reconstructive surgery,*** 119 (2): 649–661 (2007).

36. Vuillemin, T., Raveh, J., Sutter, F. J P., and surgery, reconstructive, "Mandibular reconstruction with the titanium hollow screw reconstruction plate

(THORP) system: evaluation of 62 cases", ***Plastic and reconstructive surgery ,*** 82 (5): 804–814 (1988).

37. Moiduddin, K., Anwar, S., Ahmed, N., Ashfaq, M., and Al-Ahmari, A. J I., "Computer assisted design and analysis of customized porous plate for mandibular reconstruction", ***Irbm***, 38 (2): 78–89 (2017).

38. Mensink, G., Verweij, J., Gooris, P., van Merkesteyn, J. J I. journal of oral, and surgery, maxillofacial, "Bilateral sagittal split osteotomy in a mandible previously reconstructed with a non-vascularized bone graft", ***International journal of oral and maxillofacial surgery,*** 42 (7): 830–834 (2013).

39. Poswillo, D. journal of oral surgery, "Experimental reconstruction of the mandibular joint", ***International journal of oral surgery***, 3 (6): 400–411 (1974).

40. Guyuron, B., Lasa Jr, C. I.P., and surgery, reconstructive, "Unpredictable growth pattern of costochondral graft", ***Plastic and reconstructive surgery*** , 90 (5): 880–6; discussion 887 (1992).

41. Hidalgo, D. A., Rekow, A.P., and surgery, reconstructive, "A review of 60 consecutive fibula free flap mandible reconstructions", **Plastic and reconstructive surgery,** 96 (3): 585–96; discussion 597 (1995).

42. Frodel Jr, J. L., Funk, G. F., Capper, D. T., Fridrich, K. L., Blumer, J. R., Haller, J. R., Hoffman, H. T.P., and surgery, reconstructive, "Osseointegrated implants: a comparative study of bone thickness in four vascularized bone flaps", ***Plastic and reconstructive surgery*** , 92 (3): 449–55; discussion 456 (1993).

43. Soutar, D. S., Widdowson, W. P. J H., and surgery, neck, "Immediate reconstruction of the mandible using a vascularized segment of radius", ***Head & neck surgery***, 8 (4): 232–246 (1986).

44. Ettinger, K. S., Alexander, A. E., Morris, J. M., Arce, K.J J. of O., and Surgery, M., "Novel Geometry of an Extended Length Chimeric Scapular Free Flap for Hemimandibular Reconstruction: Nuances of the Technique Streamlined by In-House Virtual Surgical Planning and 3D Printing for a Severely Vessel-Depleted Neck", ***Journal of Oral and Maxillofacial Surgery***, 78 (5): 823–834 (2020).

45. Rajan, R., Reddy, S., Rajan, R. J I. J. of O., Head, and Surgery, N., "The pectoralis major myocutaneous flap in head and neck reconstruction", ***Indian Journal of Otolaryngology and Head & Neck Surgery ,*** 49 (4): 368–373 (1997).

46. Urken, M. L., Buchbinder, D., Costantino, P. D., Sinha, U., Okay, D., Lawson, W., Biller, H. F.A. of otolaryngology–head, and surgery, neck, "Oromandibular reconstruction using microvascular composite flaps: report of 210 cases", **Archives of otolaryngology–head & neck surgery**, 124 (1): 46–55 (1998).

47. Riede, U., Lüem, M., Ilchmann, T., Eucker, M., Ochsner, P. E.J A. of orthopaedic, and surgery, trauma, "The ME Müller straight stem prosthesis: 15 year follow-up. Survivorship and clinical results", ***Archives of orthopaedic and trauma surgery***, 127 (7): 587–592 (2007).

48. Lee, S., Goh, B., Tideman, H., Stoelinga, P., and Jansen, J.I. J. O. M. S., "Modular endoprosthesis for mandibular reconstruction: a clinical, microcomputed, tomographic and histologic evaluation in 8 Macaca fascicularis", ***International journal of oral and maxillofacial surgery,*** 38: 40–47 (2009).

49. Alegret, N., Dominguez-Alfaro, A., and Mecerreyes, D.B., "3D scaffolds based on conductive polymers for biomedical applications", ***Biomacromolecules***, 20 (1): 73–89 (2018).

50. Tideman, H. and Lee, S. J A. J. O. M. S., "The TL endoprosthesis for mandibular reconstruction-a metallic yet biological approach", ***Asian J Oral Maxfac Surg,*** 18 (5): (2006).

51. Do, A., Khorsand, B., Geary, S. M., and Salem, A. K. A. healthcare materials, "3D printing of scaffolds for tissue regeneration applications", ***Advanced healthcare materials***, 4 (12): 1742–1762 (2015).

52. Mabrouk, M., Beherei, H. H., Das, D. B. %J M. S., and C, E., "Recent progress in the fabrication techniques of 3D scaffolds for tissue engineering", ***Materials Science and Engineering*** , 110: 110716 (2020).

53. Bartis, D. and Pongrácz, J.J U. P., "Three dimensional tissue cultures and tissue engineering", ***Univ Pecz,*** 11: (2011).

54. Gerhardt, L.-C. and Boccaccini, A. R., "Bioactive Glass and Glass-Ceramic Scaffolds for Bone Tissue Engineering", ***Materials (Basel, Switzerland)***, 3 (7): 3867–3910 (2010).

55. Elsayed, H., Rincón Romero, A., Molino, G., Vitale Brovarone, C., and Bernardo, E., "Bioactive Glass-Ceramic Foam Scaffolds from “Inorganic Gel Casting” and Sinter-Crystallization", ***Materials***, 11 (3): 349 (2018).

56. Zuo, W., Yu, L., Lin, J., Yang, Y., and Fei, Q., "Properties improvement of titanium alloys scaffolds in bone tissue engineering: a literature review", ***Annals Of Translational Medicine***, 9 (15): 1259 (2021).

57. Malladi, L., Mahapatro, A., and Gomes, A. S., "Fabrication of magnesium-based metallic scaffolds for bone tissue engineering", ***Materials Technology***, 33 (2): 173–182 (2018).

58. Whang, K., Healy, K. e., Elenz, D. r., Nam, E. k., Tsai, D. c., Thomas, C. h., Nuber, G. w., Glorieux, F. h., Travers, R., and Sprague, S. m., "Engineering Bone Regeneration with Bioabsorbable Scaffolds with Novel Microarchitecture", ***Tissue Engineering***, 5 (1): 35–51 (1999).

59. Gao, C., Peng, S., Feng, P., and Shuai, C. J B. research, "Bone biomaterials and interactions with stem cells", ***Bone research*** , 5 (1): 1–33 (2017).

60. Currey, J. D. J J. of M. S., "The structure and mechanics of bone", ***Journal of Materials Scienc*** , 47 (1): 41–54 (2012).

61. Heuijerjans, A., Wilson, W., Ito, K., and van Donkelaar, C. B., "The critical size of focal articular cartilage defects is associated with strains in the collagen fibers", ***Clinical Biomechanics,*** 50: 40–46 (2017).

62. Yang, Y., Wu, P., Wang, Q., Wu, H., Liu, Y., Deng, Y., Zhou, Y., and Shuai, C. M., "The enhancement of Mg corrosion resistance by alloying Mn and laser-melting", ***Materials***, 9 (4): 216 (2016).

63. Ali, D., "Mimicking Bone Anisotropic Structure with Modified Gyroid Scaffolds; A Finite Element Analysis", ***Politeknik Dergisi***, 1–1 (2021).

64. Ali, D., Ozalp, M., Blanquer, S. B., and Onel, S. E. J. of M.-B., "Permeability and fluid flow-induced wall shear stress in bone scaffolds with TPMS and lattice architectures: A CFD analysis", ***European Journal of Mechanics-B/Fluids***, 79: 376–385 (2020).

65. Sanz-Herrera, J. A. and Reina-Romo, E., "Continuum Modeling and Simulation in Bone Tissue Engineering", ***Applied Sciences***, 9 (18): 3674 (2019).

66. Egan, P., Wang, X., Greutert, H., Shea, K., Wuertz-Kozak, K., and Ferguson, S., "Mechanical and Biological Characterization of 3D Printed Lattices", ***3D Printing And Additive Manufacturing***, 6 (2): 73–81 (2019).

67. Boccaccio, A., Fiorentino, M., Uva, A. E., Laghetti, L. N., and Monno, G., "Rhombicuboctahedron unit cell based scaffolds for bone regeneration: geometry optimization with a mechanobiology – driven algorithm", ***Materials Science And Engineering: C***, 83: 51–66 (2018).

68. Ali, D. and Sen, S., "Finite element analysis of mechanical behavior, permeability and fluid induced wall shear stress of high porosity scaffolds with gyroid and lattice-based architectures", ***Journal Of The Mechanical Behavior Of Biomedical Materials***, 75: 262–270 (2017).

69. Zysset, P. K., Guo, X. E., Hoffler, C. E., Moore, K. E., and Goldstein, S. A., "Elastic modulus and hardness of cortical and trabecular bone lamellae measured by nanoindentation in the human femur", ***Journal Of Biomechanics***, 32 (10): 1005–1012 (1999).

70. Hamed, E., Jasiuk, I., Yoo, A., Lee, Y., and Liszka, T., "Multi-scale modelling of elastic moduli of trabecular bone", ***Journal Of The Royal Society Interface***, 9 (72): 1654–1673 (2012).

71. Pinto, V., Ramos, T., Alves, S., Xavier, J., Tavares, P., Moreira, P., and Guedes, R., "Comparative failure analysis of PLA, PLA/GNP and PLA/CNT-COOH biodegradable nanocomposites thin films", ***Procedia Engineering***, 114: (2015).

72. Ng, C. C., Savalani, M. M., Lau, M. L., and Man, H. C., "Microstructure and mechanical properties of selective laser melted magnesium", ***Applied Surface Science***, 257 (17): 7447–7454 (2011).

73. Gómez, S., Vlad, M. D., López, J., and Fernández, E., "Design and properties of 3D scaffolds for bone tissue engineering", ***Acta Biomaterialia***, 42: 341–350 (2016).

74. Li, C.-H., Wu, C.-H., and Lin, C.-L., "Design of a patient-specific mandible reconstruction implant with dental prosthesis for metal 3D printing using integrated weighted topology optimization and finite element analysis", ***Journal Of The Mechanical Behavior Of Biomedical Materials***, 105: 103700 (2020).

75. Yan Choy, H., Sheng Tan, P., and Woon Choy, K., "Finite Element Analysis of Open Reduction Internal Fixation for Mandible Fracture", ***ICBET '21: 2021 11th International Conference on Biomedical Engineering and Technology***, Tokyo Japan, (2021).

76. "MCA | Free Full-Text | A Transdisciplinary Approach for Analyzing Stress Flow Patterns in Biostructures", **https://www.mdpi.com/2297-8747/24/2/47** (2022).

77. Pałka, Ł., Kuryło, P., Klekiel, T., and Pruszyński, P., "A mechanical study of novel additive manufactured modular mandible fracture fixation plates - Preliminary Study with finite element analysis.", ***Injury***, 51 (7): 1527–1535 (2020).

78. Luo, D., Xu, X., Guo, C., and Rong, Q., "Fracture Prediction for a Customized Mandibular Reconstruction Plate with Finite Element Method", ***In Advanced Computational Methods in Life System Modeling and Simulation***, (2017).

79. Manakari, V., Parande, G., and Gupta, M., "Selective Laser Melting of Magnesium and Magnesium Alloy Powders: A Review", ***Metals***, 7 (1): 2 (2017).

80. Kowalczyk, M., Piorkowska, E., Kulpiński, P., and Pracella, M., "Mechanical and thermal properties of PLA composites with cellulose nanofibers and standard size fibers", ***Applied Science and Manufacturing***, (2011).

81. Li, B. and Aspden, R. M., "Composition and Mechanical Properties of Cancellous Bone from the Femoral Head of Patients with Osteoporosis or Osteoarthritis", ***Journal Of Bone And Mineral Research***, 12 (4): 641–651 (1997).

RESUME

Ammar Hussen Farag Idres graduated first and elementary education in Yemen. He completed high school education in Kuwait High School; after that, he started the undergraduate program in Karabük University Department of Biomedical Engineering in 2015. Then in 2019, he started working as a biomedical sales engineer in EMS mobile systems ambulance factory. At the same time, he started doing his master's degree in biomaterial science at Karabuk University.